SLAC-PUB-3343
May 1984
(A)

ELECTRON LINEAR ACCELERATORS AND STRETCHERS*

GREGORY A. LOEW
Stanford Linear Accelerator Center
Stanford University, Stanford, California 94305

Introduction

The need for high duty factor electron accelerators in the Nuclear Physics community is not new. In recent years, however, this need has given birth to a large number of projects. Some of these projects are extensions of existing machines to higher duty factor, others are entirely new accelerator complexes. In the USA, in addition to existing low energy projects, several institutions were until recently competing with each other for the opportunity to build the "ultimate" electron machine in the 0.5 → 6 GeV energy range. Finally, in April 1983, the electron linac-stretcher ring proposed by the Southeastern Universities Research Association (SURA) was selected among several technical projects as the best candidate to fulfill this goal. Similarly, in other countries, a number of institutions are either embarking on upgrading existing facilities or building new ones. All these projects are pinpointed geographically in Fig. 1.

One of the remarkable features about Fig. 1 is the preponderance of linear accelerator-pulse stretcher ring projects, namely: EROS (Saskatoon), SURA, possibly MIT, Saclay, NIKHEF (Amsterdam), Frascati, Kharkov and the two Tohoku University (Sendai) projects, one a prototype already built, the other proposed. The other projects belong to different categories of accelerators which will be described briefly below.

Options for High Duty Factor Electron Accelerators

The fact that electron linacs coupled to pulse stretcher rings have become so prevalent is of course not a coincidence. The reasons are several:

1. For those laboratories which already have a linac, adding a stretcher is a natural next step, even if the linac has to be modified somewhat as one couples it to the ring.
2. The requirements of Nuclear Physics have not only evolved towards higher duty factor, they have also risen to higher energies. As the energy has increased above 1 GeV, the other technical candidates such as microtrons have become increasingly difficult to build.
3. Other technological approaches, such as superconducting linacs, which looked very appealing a few years ago, have not lived up to their promises so far.

---

*Work supported by the Department of Energy, contract DE-AC03-76SF00515.

Invited Lecture presented at the INS-Kikuchi Winter School on Accelerators for Nuclear Physics, Fujiyoshida, Japan, January - February 1, 1984.

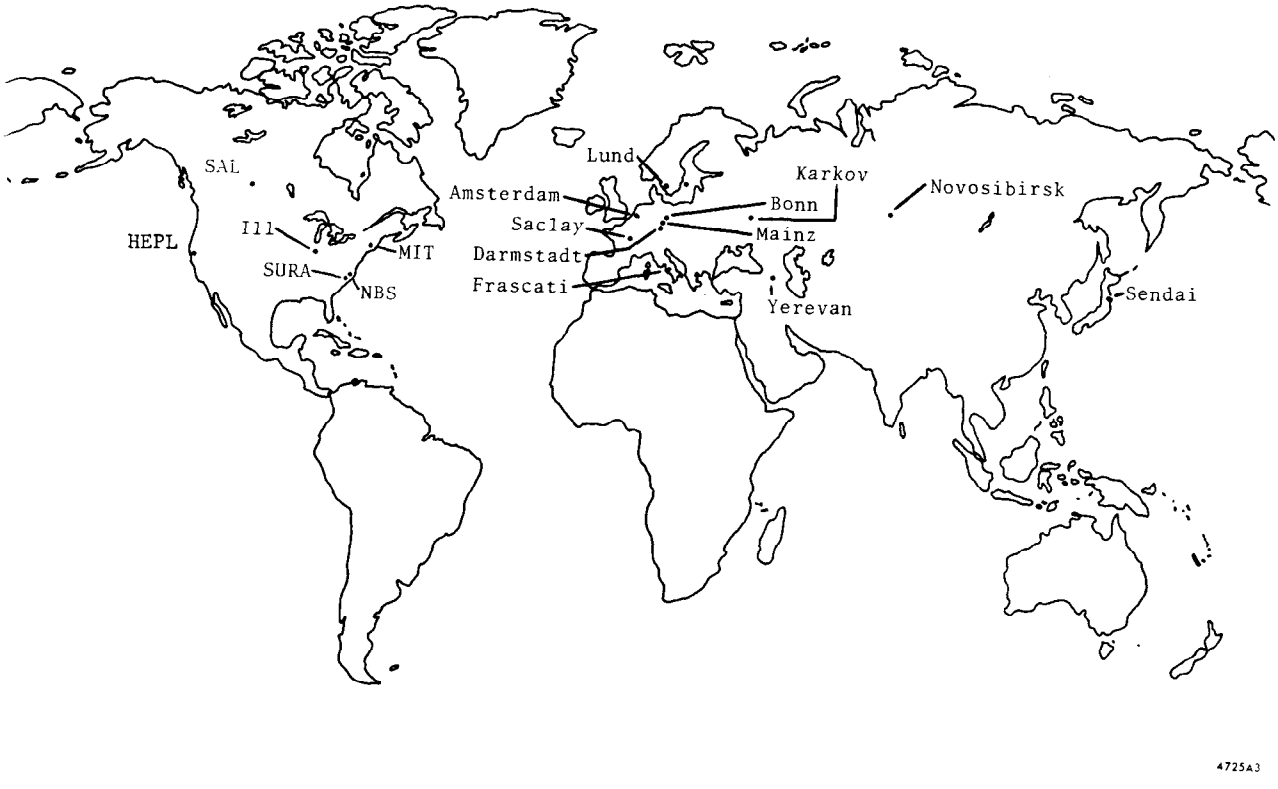

Figure 1. High duty factor electron accelerator projects in the world.

In spite of these developments, before we go on to describing the basic principles of linacs and stretchers, it seems educational to review the other options. When one looks for high duty factor machines for fixed target experiments, only two basic schemes come to mind: either the acceleration and extraction of the beam are continuous and follow each other directly, or they are separated by some intermediate storage in a device such as the stretcher ring. In the first case, one needs a cw linac. This linac can either be a straight multi-section machine through which the beam passes only once, or it can be a one-, two- or three-section machine with a guide magnetic field which allows many recirculating orbits (this is the microtron), or it can be a multi-section linac of intermediate length through which the beam is recirculated a few times by means of independent magnetic channels. These three basic schemes are illustrated in Fig. 2. In the second case, the acceleration is done in a pulsed manner for a large number of particles which are stored at once in a ring from which they are then extracted gradually. The acceleration can be obtained in a pulsed microtron, in a synchrotron or preferably in a linac, as shown in Fig. 3.

One of the key characteristics of the accelerators shown in Fig. 2 can be understood in terms of the following simplified power balance equation[1] derived from the definition of the shunt impedance rL of a linac of length L and voltage gain V:

$$rL = \frac{V^2}{P_{lost}} \tag{1}$$

where P_{lost} is the RF power lost in the walls of the structure. Then, for a duty factor D, the time-average RF power supplied to the accelerator is

$$P_{RF} = \frac{D\,V^2}{rL} + P_{beam} \tag{2}$$

where $P_{beam} = V\,i_{ave}$ and i_{ave} is the average beam current. To get a feeling for the order of magnitude of the numbers we are considering, let us assume that we are trying to design a multi-section linac (Fig. 2a) with unity duty factor ($D = 1$), $V = 4$ GV and $i_{ave} = 250\ \mu$A, i.e., $P_{beam} = 1$ MW. A realizable value of the shunt impedance per unit length r at S-band is $80 \times 10^6\ \Omega/m$. We see that

$$P_{lost} = \frac{2 \times 10^5}{L}\ \text{MW} \quad .$$

Thus, even if we were willing to build a 2 km linac, we would still lose 100 MW of RF power to the walls alone. Given typical conversion efficiencies from ac to RF power of at best 50% in a cw regime, we would need over 200 MW of power, which would be prohibitive. In addition, it would take 200 0.5 MW-klystrons, and the power dissipation in the structure would be 50 kW/m, which is not easy to handle. This approach is thus not practical.

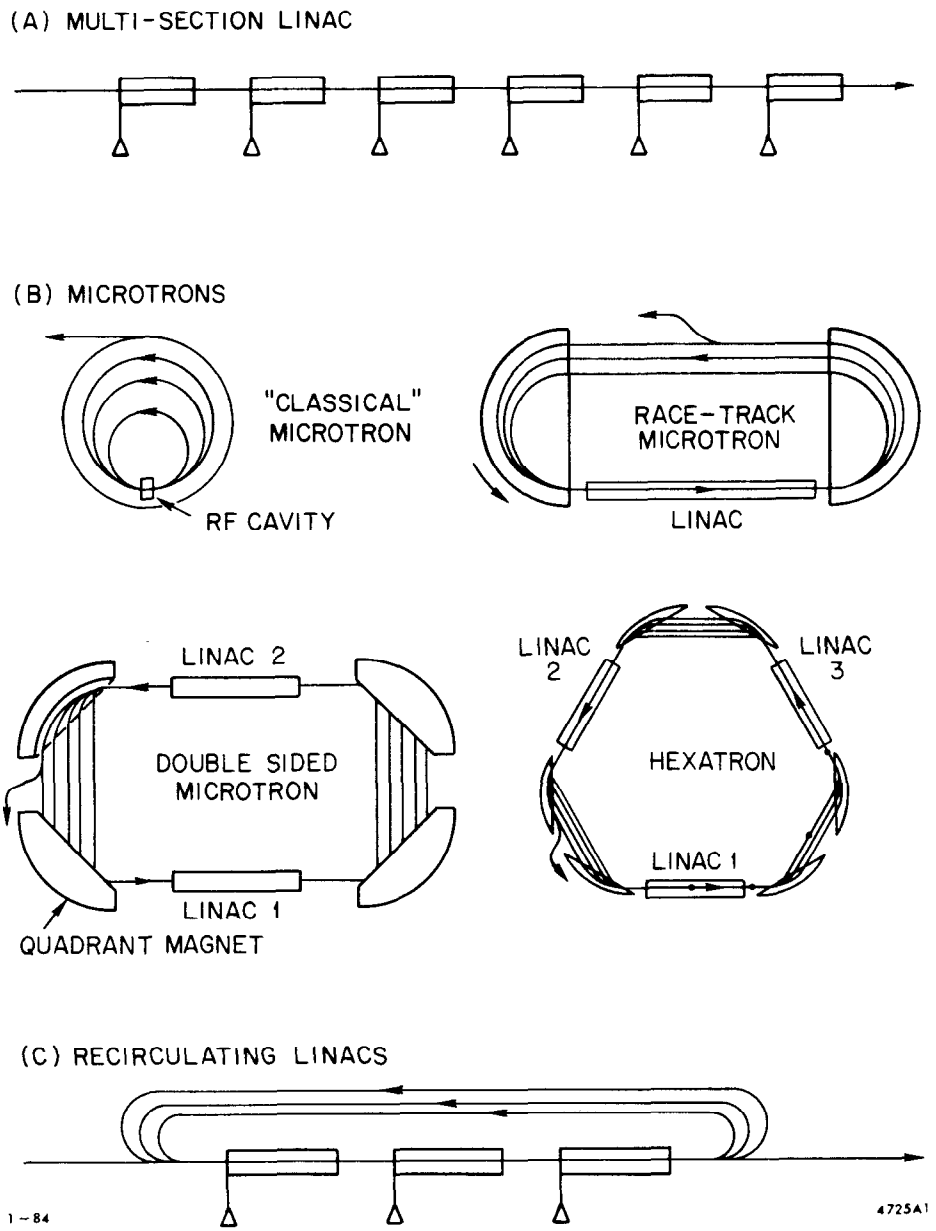

Figure 2. Schemes in which acceleration and extraction are continuous and follow each other directly.

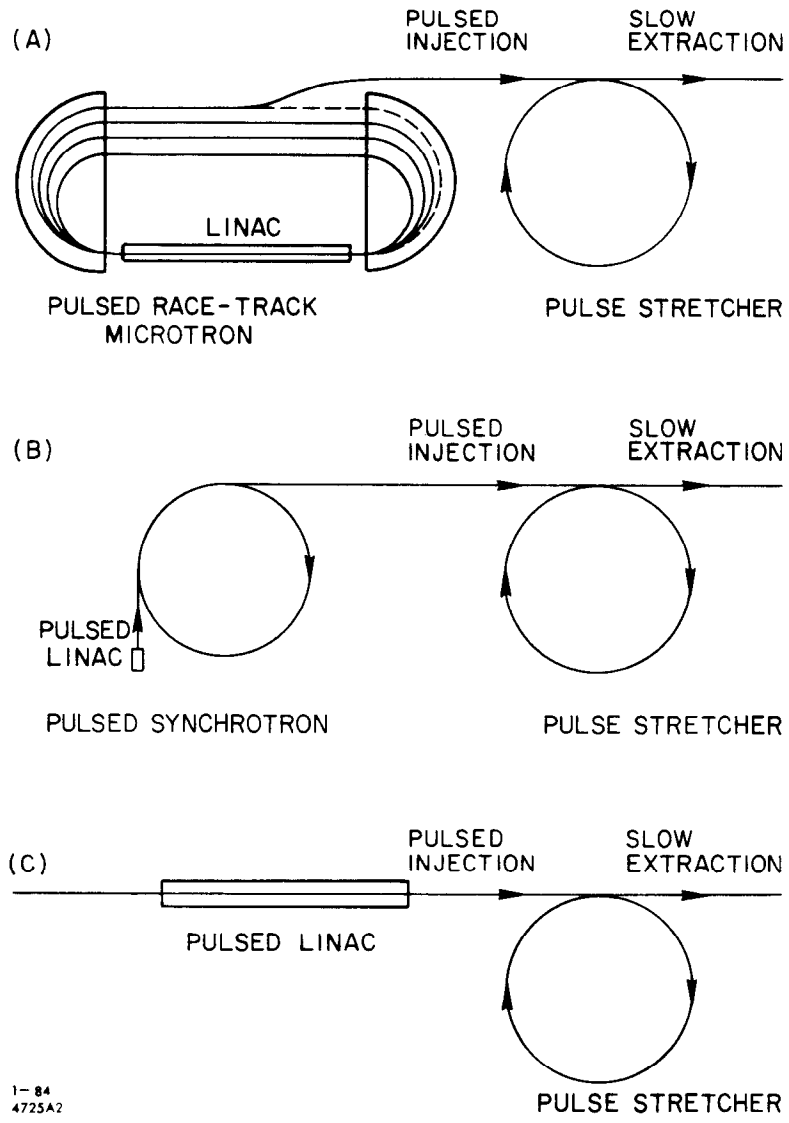

Figure 3. Schemes in which acceleration and extraction are separated by an intermediate storage.

It was this obstacle which in the 1960's gave a major impetus to the field of RF superconductivity. The original hope was to reach gradients of 20-30 MV/m and Q-improvement factors of $\sim 10^5 - 10^6$ at 1.8° K. In actual fact, RF superconductivity turned out to be a much more difficult field than expected and even today, cw gradients of 4 MV/m and Q-improvement factors of 5×10^4 are barely reachable in long structures. Assuming, however, that they could be obtained, a 4 GeV superconducting accelerator would be 1 km long. The RF losses at 1.8° K would be reduced to 4 KW (instead of 100 MW!) and the RF sources would predominantly supply the 1 MW beam power. Thus the power consumption of the accelerator would be considerably reduced. Even with a refrigeration system with an efficiency of 2×10^{-3} and a Dewar with a static loss of 1 watt/m at 1.8° K, the refrigerator would consume only 2.5 MW. Unfortunately, the complexity and cost of such a linac would be enormous: a not untypical cost of $\$10^5$/m of cooled structure would result in \$100 million for the accelerator alone, and the reliability might be questionable. Also, it is not clear from experience with superconducting structures that an average current much beyond 100 μA would be achievable because of beam breakup due to excitation of higher order modes. Thus, a 4 GeV multi-section superconducting linac does not seem practical either.

The realization of these facts prompted many accelerator designers, particularly at lower energies, to favor the idea of recirculating the beam through the accelerating structure. If the number of recirculations is N, then for the same final energy V, the energy gain needs to be only V/N and Eq. (2) becomes

$$P_{RF} = \frac{D\,V^2}{rL\,N^2} + P_{beam} \tag{3}$$

where the power lost is reduced by N^2. All the microtrons (Fig. 2b) and recirculating linacs (Fig. 2c) are motivated by this simple observation.

Of the microtrons indicated in Fig. 1, the first cw race-track microtron which became operational (1972) is the one at the University of Illinois.[2] It currently operates with a superconducting 6 meter, 12 MeV section (made at HEPL, Stanford), and with 6 traversals, it reaches energies up to 70 MeV. Its current, however, is limited to 1 μA by beam breakup. In the future, the end magnets will be replaced by new ones and the superconducting section may be replaced by a room temperature one. These improvements should upgrade the facility to 200 MeV and a higher average current.

The second cw race-track microtron in Fig. 1 is the one at the University of Mainz (MAMI).[3] It presently consists of two cascaded stages. The first stage has been operational since 1979. With a Van de Graaf injector at 2.1 MeV, 20 traversals through a room temperature section with 0.6 MeV/turn, it has reached an output energy of 14 MeV. The second stage has been operational since 1983 with 51 turns through a room temperature

section with 3.1 MeV/turn and an output energy of 175 MeV. Total power consumption is 240 kW. The average output current under operating conditions is approximately 30 μA. A third stage up to 800 MeV may be forthcoming later.

The third cw race-track microtron in Fig. 1 is the first stage (RTM-1) of the National Bureau of Standards project[4] in Washington, D.C. It is presently under construction and should come into operation in October 1985. With an input energy of 5 MeV, 16 passes through a room temperature section with 12 MeV/turn, this machine is expected to produce an output energy of up to 200 MeV. It is hoped that the average design current will be in excess of 300 μA. Indications are that the beam breakup effect will not be nearly as severe as in superconducting structures. This first stage, RTM-1, was to be followed by a second stage, RTM-2, capable of going up to 1 GeV. This expansion, however, was not approved.

The Hexatron in Fig. 2, proposed by the Argonne National Laboratory,[5] was the main competitor for the future U.S. 4 GeV high duty factor machine together with the SURA linac-stretcher project. The Hexatron was a modification of a conventional race-track microtron that would make it possible to attain much higher energies than previously attainable with microtrons. The design involved 37 orbits with a high energy gain per turn (105 MeV) and a large orbit separation (17 cm). The Hexatron was to use a 23 MeV linac cascaded with an intermediate 185 MeV race-track microtron as an injector. The acceleration in the Hexatron was to be produced by three linacs as shown, each 25 m long with an energy gain of 35 MeV and a total of 66 cw 50 kW klystrons at 2400 MHz. The specified average current was to be 300 μA which could be shared among a maximum of three separate extracted beams at different energies. The design of the Hexatron at 4 GeV was considered competitive in most ways with the SURA proposal but the DOE-NSF Nuclear Science Advisory Committee (NSAC) which had to make the final choice, after considerable deliberation gave preference to the SURA machine. Some of the reasons given were that the magnetic guide-field uniformity and position tolerances of the sector magnets may have been hard to meet, that quantized synchrotron radiation above 3.5 GeV may have given emittance problems resulting in the need for large linac apertures (greater than the planned 1.2 cm diameter, which would have resulted in lower shunt impedances and more RF power) and that the desired extension in energy to 6 GeV would not have been possible.

The third category of machines shown in Fig. 2c, namely recirculating cw linacs, makes use of the same basic idea as the microtrons, namely economy of RF power and accelerator length, by increasing the number of passes from 1 to N. By using independent magnetic channels rather than single uniform-field end-magnets, the restriction between energy gain, magnetic field and orbit length is removed. However, it is not trivial to obtain

a large number of passes, both from the point of layout and beam breakup limitations. The latter difficulty arises particularly if the linacs are superconducting. There are only two cw recirculating accelerators in the world: the first one at Stanford (HEPL) is operational, the second one at Darmstadt is under early construction. The HEPL machine uses its 1300 MHz superconducting linac (SCA) which produces electrons with 70 MeV/pass at a duty factor between 0.1 and 1 (limited by the capability of the refrigeration system). In the recirculating mode (SCR), up to three passes for a total of 200 MeV are obtained in practice. The maximum average currents achievable are 500 μA for 1 pass, 100 μA for 2 passes and 20 μA for 3 passes.[6] The beam breakup onset time depends of course on the current but has been observed as early as 1 msec after injector turn on. The Darmstadt machine, presently under joint construction with the University of Wuppertal which is responsible for the superconducting linac, is being designed for 40 MeV/pass and a maximum of 3 passes and 130 MeV. The design current is 20-30 μA. As we see, neither of these accelerators has been designed for very high energy, certainly not the 4 GeV level desired for the next generation of high duty factor machines. The cost and complexity of the superconducting linacs which constitute the main building block of these installations have obviously created a barrier difficult to overcome.

We now come to the machines in Fig. 3 in which acceleration is separated from extraction by an intermediate storage. Before we proceed to the cases under Fig. 3c which are the main topic of this lecture, let us briefly consider the cases under Fig. 3a and 3b. The only example of a pulsed race-track microtron for injection into a stretcher ring is the MAX accelerator at the University of Lund in Sweden.[7] The race-track microtron is designed for an energy of up to 100 MeV, 750 pps, a peak current of 25 mA for a pulse length of 2 μsec and an energy spread of $\pm 0.1\%$. The stretcher ring has a magnetic bending radius of 1.2 m and a circumference of 18.75 m. Multi-turn injection can be used during the 2 μsec injection time after which slow extraction can proceed in the interpulse time of the microtron. The ring in its original design for the stretcher mode was to work without RF system. A 4/3 horizontal resonance excited by sextupole magnets is to be used for the extraction during each 1.33 ms period. In another mode used for internal tagging, the beam is to be accelerated in the ring to 500 MeV by a 400 MHz RF system. The ramping up is to take 1 s followed by a 20 s spill.

Referring to Fig. 3b, there are two stretcher projects which use synchrotrons as injectors, ELSA now under construction at the University of Bonn,[8] and possibly a project at Yerevan in the U.S.S.R. The ELSA stretcher ring will receive its electrons from the Bonn 2.5 GeV synchrotron which has an accelerating cycle of 20 ms (50 pps). At the end of this cycle, the beam will be transferred to the stretcher. The ring has a circumference of 164 m, about 2.35 that of the synchrotron, and it will be filled up to a circulating intensity of 5×10^{10} electrons by a three-turn extraction from the synchrotron. The ring will have

a 500 MHz RF system, both for the stretcher storage mode and for an accelerating mode in which the ring will be ramped from 1.75 to 3.5 GeV maximum. Extraction will be achieved by a third integer resonance. Note that in comparison with the stretchers using linac injectors which will be discussed below, the extracted intensity (a few μA) is comparatively low, both because the charge available from the synchrotron is low and because the synchrotron is limited in the number of pulses per second to about 50. In contrast to the injection from a pulsed linac which is turned off during extraction from the stretcher, the synchrotron is on and getting ready for the next fill of the ring.

There has also been occasional information coming from the U.S.S.R. that the 6 GeV Yerevan electron synchrotron might be outfitted with a storage ring for beam stretching and synchrotron light generation. The author, however, lacks any pertinent information on this project.

Similarly, at Novosibirsk, the VEPP storage rings have been used to do some experiments using internal targets. While this work cannot quite be compared with building a high duty factor accelerator, it is sufficiently similar to be worth mentioning.

Linac-Stretcher Design Criteria

The nine* linac-stretcher complexes mentioned in the introduction have many features in common. Typically, as shown in Fig. 4, they all consist of a conventional pulsed linac of fairly low duty factor equipped with traveling-wave accelerator sections driven by high power klystrons and modulators. If necessary, a beam recirculation system is used to double the energy. At the end of the linac, there is often an energy compression system (ECS) to concentrate the electrons into a narrow $\Delta E/E$ spectrum. The linac is followed by a transport system which delivers the pulsed train of intense electron bunches to the stretcher ring. Injection is achieved by a system of septa and kickers. In many cases, although not all, a single-turn injection is used and the beam is placed directly on the equilibrium orbit, which causes the stored beam size to be as small as possible and instabilities to be reduced. This in turn can reduce the emittance of the extracted beam. Extraction starts as soon as possible after injection and is designed to last the entire interpulse period. All machines use either a 1/3 or 1/2 resonant extraction technique. The goal is to obtain a duty factor as close to 1 as possible (typically 0.9). Depending on the design and physics possibilities, one or more beams are extracted and sent to experimental end-stations.

---

*For lack of information, there will be no discussion in this paper of the Kharkov machine. Nor will there be any discussion of the MIT option to upgrade the Bates linac capabilities by means of a stretcher because their plans are presently in a state of flux.

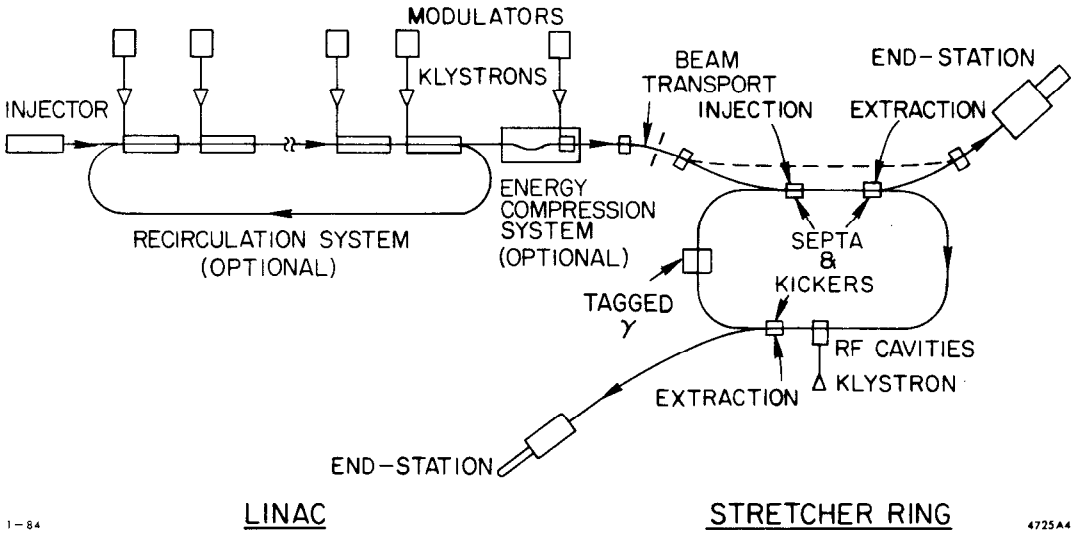

Figure 4. Layout of a typical linac-stretcher complex.

Aside from inevitable variations in style, space and ideas from laboratory to laboratory, the differences between the various projects arise from their different energies and above all, from their different histories. Of all the machines in the planning stage, only Frascati, SURA, and the future Tohoku University machine benefit from the luxury of starting from a fresh linac design, unhampered by earlier constraints.

Given below are some of the basic design rules and criteria.

— For a high duty factor out of the stretcher, the linac energy must be equal to the ring operating energy, i.e., no time for acceleration in the ring is allowed.

— For single-turn injection on the equilibrium orbit, the linac beam pulse is chosen to be equal or almost equal to the going-around time of the stretcher (see Fig. 5). The only limitation to equating the two is the fall-time of the injection kicker (see below). This effect produces a small gap in an otherwise continuous train of bunches.

— Neglecting the small gap, the maximum average current i_S obtainable from the stretcher is simply

$$i_S = I_L \, D_B \tag{4}$$

where I_L is the peak current out of the linac and D_B is the linac beam duty cycle (not to be confused with the RF duty cycle D_{RF} of the linac).

— Generally, one starts out with a requirement given by the nuclear physicists on the desired value of i_S and one looks at the design implications for I_L and D_B. The value of I_L is the value of both the peak linac current (which one wants to make as large as possible but which is limited by linac beam loading and break-up) and the initial current in the ring (which is also limited by ring instabilities but which decays linearly during extraction). The duty factor D_B is given by

$$D_B = t_B \, n_{pps} \tag{5}$$

where t_B is the linac beam pulse length and n_{pps} is the linac repetition rate. If we let R be the magnetic radius of the ring and p be the "packing" factor of the ring (always greater than 1) such that the circumference of the ring is $2\pi pR$, then

$$D_B = \frac{2\pi pR}{c} \, n_{pps} \tag{6}$$

and the charge delivered per linac pulse is

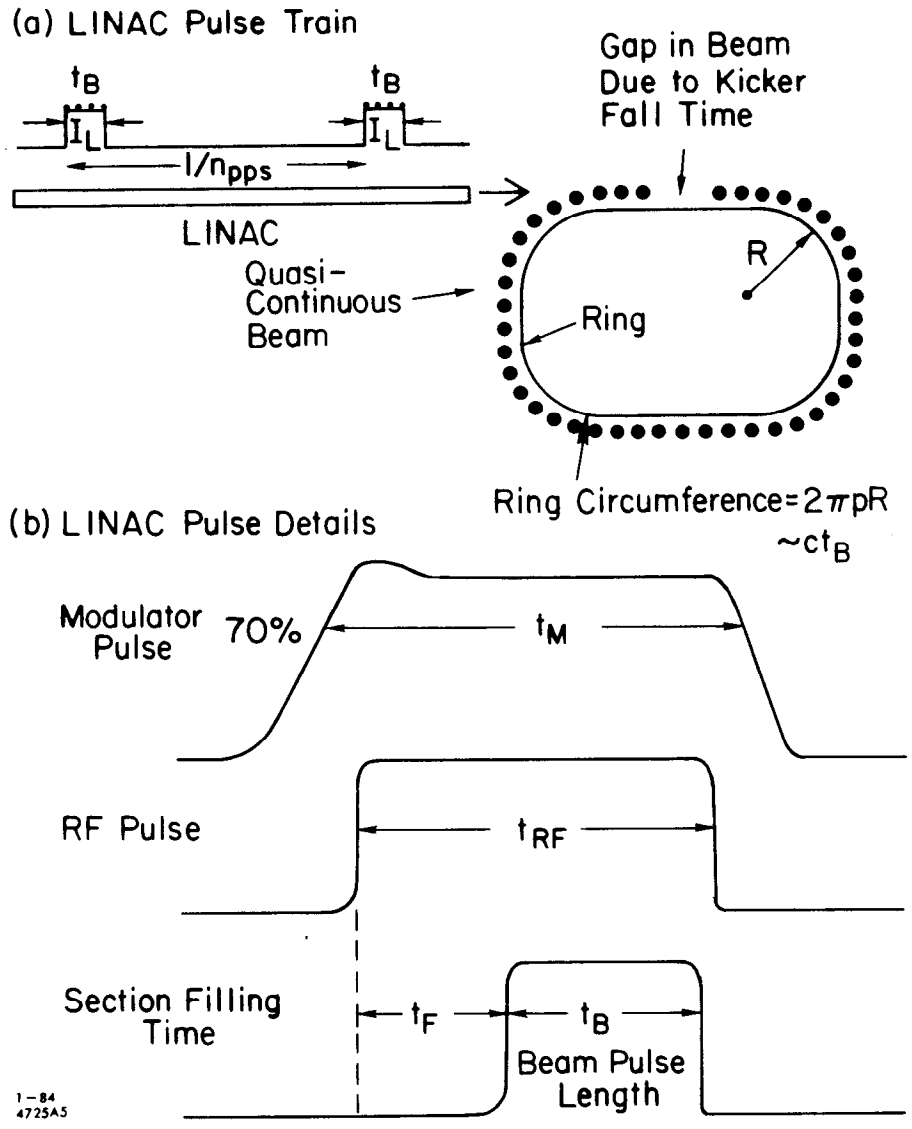

Figure 5. Pulse relationships in the linac and the stretcher.

$$Q_L = I_L \frac{2\pi pR}{c} \tag{7}$$

where c is the velocity of light. Expression (4) can also be written as

$$i_S = I_L \frac{2\pi pR}{c} n_{pps} \tag{8}$$

$$= I_L t_B n_{pps} \tag{9}$$

$$= Q_L n_{pps} \quad . \tag{10}$$

All these equations may seem trivial but they express many of the fundamental trade-offs which must be made to converge on a practical design. The theory of beam break-up in linacs shows[9] that for beam pulse lengths in the μsec range, the quantity Q_L is roughly conserved for a linac of given length, gradient and focusing. Thus from Eq. (10), the obtainable i_S scales directly with n_{pps}. However, n_{pps} is not a totally free parameter because above a certain repetition rate, the modulators which drive the klystrons have insufficient time to recharge and the thyratrons which are used as switch tubes begin to run into difficulties. Equations (8) and (9) show that if we limit I_L because of beam loading and n_{pps} because of the reasons given above, then our only free parameter is the linac beam pulse length and by inference the ring circumference. It may be argued that enlarging the ring is good because it makes it easier to build, enlarges the magnetic radius, reduces the magnetic field for a given energy and therefore reduces both the energy loss due to synchrotron radiation and the power consumption to excite the magnets. It turns out, however, that the power consumption of the ring is a small fraction of the power consumption of the linac and that in any case, this cost saving would be offset by the increased capital cost due to the ring size. Furthermore, a longer linac beam pulse length implies a longer klystron and modulator pulse. Recent results with klystron tests at SLAC indicate that klystrons run into breakdown and possibly window difficulties when the pulse length exceeds 3 or 4 μsec. Since the RF pulse length t_{RF} is given by

$$t_{RF} = t_F + t_B \tag{11}$$

and in case of one recirculation of the beam in the linac (i.e., two passes),

$$t_{RF} = t_F + 2t_B \quad , \tag{12}$$

where t_F is the filling time of the accelerator, lengthening t_B runs into limits of its own even if I_L is decreased accordingly to conserve Q_L.

— It was mentioned earlier that beam loading has a limiting effect on the allowable value of I_L. Conversely, referring to Eq. (4), we see that quite independently of all the other remarks already made, increasing D_B has a direct effect on D_{RF} since

$$D_{RF} = D_B + t_F n_{pps} \tag{13}$$

and D_{RF} affects both the capital equipment costs of the klystrons, modulators and accelerator cooling systems, as well as the operating costs.

Actual Designs of Linac-stretcher Projects

We will now summarize by means of a table and a set of figures how the various institutions interested in building linac-stretcher projects are coping with the above design criteria and compromises. Shown in Table 1 are the various machines for which information is available to the author at this time. The listing is given in order of ascending energy from left to right.

The only machine presently in operation is the SSTR linac-stretcher at Tohoku University.[10] It is shown with actual operating results in the first column of Table 1 and in the set of Figs. 6. Note that it does not have an RF system. This pilot machine, the first of its kind, is providing valuable learning experience to the entire community and in particular to the staff of Tohoku University which is proposing to build a much larger project (see sixth column).

The EROS machine parameters[11] are listed in the second column and the layout is shown in Fig. 7. The linac has been in existence for more than twenty years and the EROS project was proposed as early as 1974. It has recently been funded. As can be seen, the stretcher has the shape of a race-track and it will be built in the existing linac tunnel.

The NIKHEF machine[12] in the third column is under early study. Its layout is also being adapted to the existing linac tunnel. As shown in Figs. 8, it is presently conceived with one loop at each end joined by two long straight sections, making it the stretcher with the largest circumference (1.7 μsec going-around time). A 6-turn injection scheme is being proposed, which is well adapted to the long beam pulses of the NIKHEF linac. Extraction studies are underway but a final scheme has not yet been chosen. This project has not yet been funded but its future seems to be fairly secure.

The Frascati project (ALFA 3)[13] is a multi-purpose machine with several goals: high duty factor nuclear physics with electrons and photons, monochromatic and polarized photon physics from a backscattered laser up to 400 MeV, synchrotron light from superconducting wigglers, and high intensity neutron spectroscopy. The linac does not exist at this time and will have to be procured when the project is approved. The timetable for

Table 1
SUMMARY OF LINAC-STRETCHER PARAMETERS

	SSTR (Tohoku)	EROS (Saskatoon)	NIKHEF (Amsterdam)	FRASCATI (Italy)	SACLAY (France)	STR (Tohoku)	SURA (Virginia)
Overall System	(Actual Results)						
Energy range (GeV)	0.1 → 0.15	0.1 → 0.3	0.1 → 0.5	0.3 → 1.1	0.5 → 1.3	0.3 → 3.3	0.5 → 4 → 6
Duty cycle	0.8	0.8	0.8	0.9	0.8	>0.9	>0.9
Extracted current	1μA	72μA	50μA	100μA	100μA	70/140μA	240μA
Linac							
Peak Energy (one pass)	0.380 GeV	0.3 GeV	0.5 GeV	1.1 GeV	1.75 GeV	2.0 GeV	2.2 GeV
Peak Current, I_L	140 mA	200 mA	50 mA	160 mA	200 mA	200 mA	200 mA
Beam pulse length	20 nsec, 100 nsec	0.3, 1 μsec	10.2 μsec	3.1 μsec	1 μsec	1.2 μsec	1.2 μsec
RF pulse length	3.5 μsec	2.5 μsec	12 μsec	4.2 μsec	2.4 μsec	≤ 4.2 μsec	3.2 μsec
Repetition rate	100-300 pps	360 pps	1000 pps	200 pps	500 pps	300 pps	1000 pps
Beam duty cycle	0.03×10^{-3}	0.36×10^{-3}	10.2×10^{-3}	0.62×10^{-3}	0.5×10^{-3}	0.36×10^{-3}	1.2×10^{-3}
Overall length	54 m	~ 30 m	~ 200 m	>110 m	174 m	238 m	158 m
Number of sections	21	7	24	24	24	32	36
Frequency	2856 MHz	2856 MHz	2856 MHz	2856 MHz	2998.5 MHz	2856 MHz	2856 MHz
Number of klystrons	5	6	12	12	24	28	36
Klystron peak power	~ 20 MW	~ 20 MW	2 → 4 MW	30 MW	25 MW	40 MW	40 MW
Number of passes through linac	1	1	1	1	1, possibly 2 later	possibly 2	possibly 2
Emittance ($\pi \cdot \frac{MeV}{c} \cdot cm$)	0.013	not known	0.012	0.030	0.013	0.030	0.020
$\Delta E/E$	0.1 → 2%	0.2 → 1%	0.3%	0.1 → 2%	0.1 → 1%	0.1 → 2%	0.2%
Energy Compression System (ECS)	yes	yes	probably	probably	yes	yes	yes
Stretcher							
Circumference, $2\pi pR$	15.47 m	~ 108 m	510 m	460.77 m	300 m	382.8 m	382.7 m
Magnetic radius, R	0.8 m	1 m	Firm details	22.3 m	15 m	16.7 m	26.85 m
Packing factor, p	3.07	17.18	not yet available	3.28	3.18	3.45	2.14
Maximum bending magnet field	0.62 T	1 T	↓	0.16 T	0.28 T	0.65 T	0.5 T
Number of bending magnets	8	8	↓	48	64	32	32 + 12
Number of quadrupoles	1	26 + 10	↓	204	100	not known	30 + 20 + 14
Number of sextupoles	1 + 1	10 + 2	↓	6	not known	not known	16
Betatron tunes ν_x, ν_y	1.22, 1.28/1.3, 1.2	4.2633, 4.8	↓	17.33, 7.25	8.5, 8.6	9.5, 9.4	8.5, 8.8 (variable)
RF System				Not			
Frequency	—	~ 714 MHz	yes	used in	~ 600 MHz	476 MHz	714 MHz
Voltage		90 kV at 300 MeV		stretcher mode	600 kV		4.5 MV variable 1.5 MV continuous
Power					40 kW	400 kW	5/350 kW
Injection method	2-turn and multi-turn horizontal	1- or 3-turn horizontal-vertical	6-turn horizontal	2-turn horizontal	1-turn horizontal	1-turn	1-turn vertical
Extraction Method	$\frac{1}{3}$ resonance monochromatic	$\frac{1}{2}$ resonance, achromatic $\frac{1}{3}$ resonance, monochromatic	$\frac{1}{3}$ resonance or $\frac{1}{2}$ resonance	$\frac{1}{3}$ resonance monochromatic	$\frac{1}{2}$ resonance achromatic	$\frac{1}{2}$ resonance achromatic	$\frac{1}{2}$ resonance achromatic
Emittance (π mm·mrad)							
x	5	1	not yet defined	4	0.5	0.5	0.3
y	3	1		4	0.1	1.0	0.1
$\Delta E/E$	0.2%	0.1%		0.02%	0.1%	0.1%	0.2%

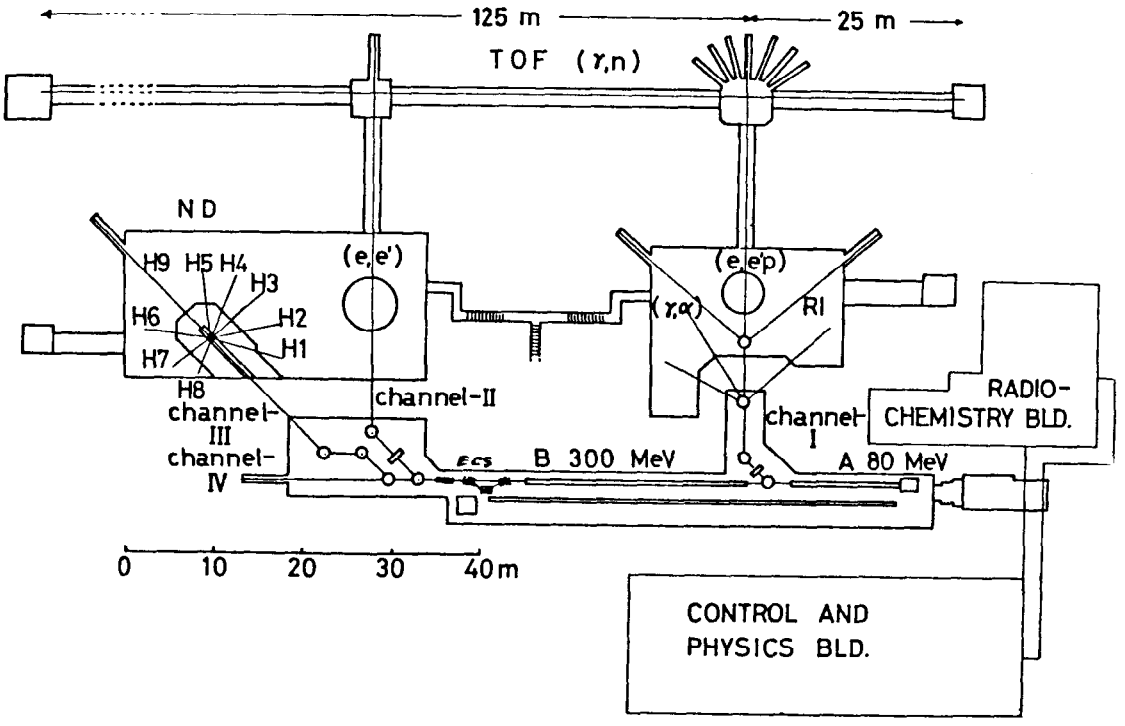

Figure 6a. General layout of 380 MeV Tohoku electron linac.

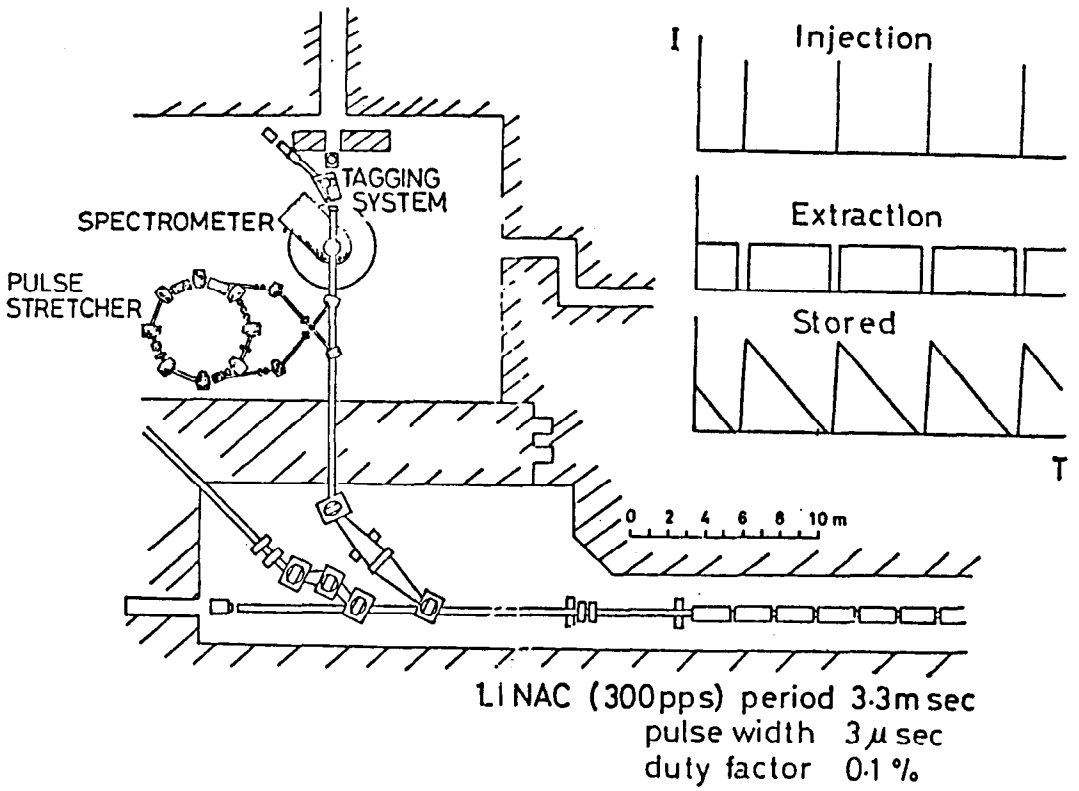

Figure 6b. Layout of Tohoku SSTR in experimental area at end of linac.

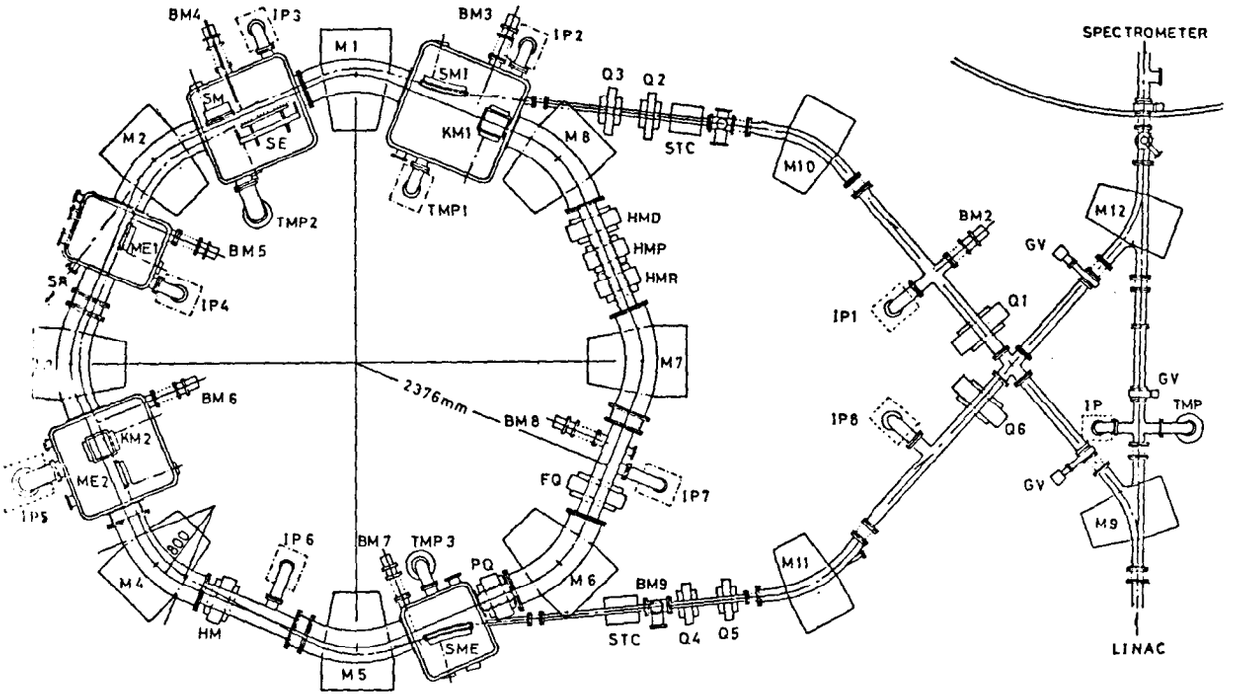

M: bending magnet
Q,FQ: quadrupole mag.
PQ: pulsed quadrupole m.
HM: sextupole mag.
KM: bump mag.

SM,SMI:septum mag. for inj.
ME,SME:septum mag. for extr.
SE: septum electrode
BM: beam profile monitor
SR: synchrotron light moni.

GV: gate vulve
IP: spatter ion pump
TMP:turvo molecular p.
STC: stearing coil

Figure 6c. Details of SSTR layout.

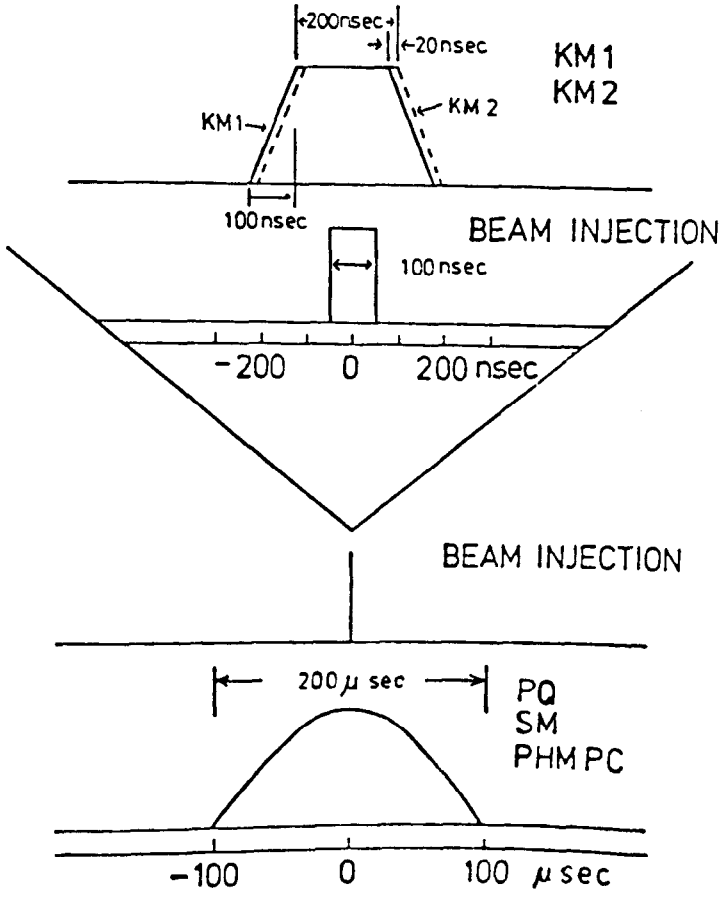

Figure 6d. Timing sequence of SSTR injection.

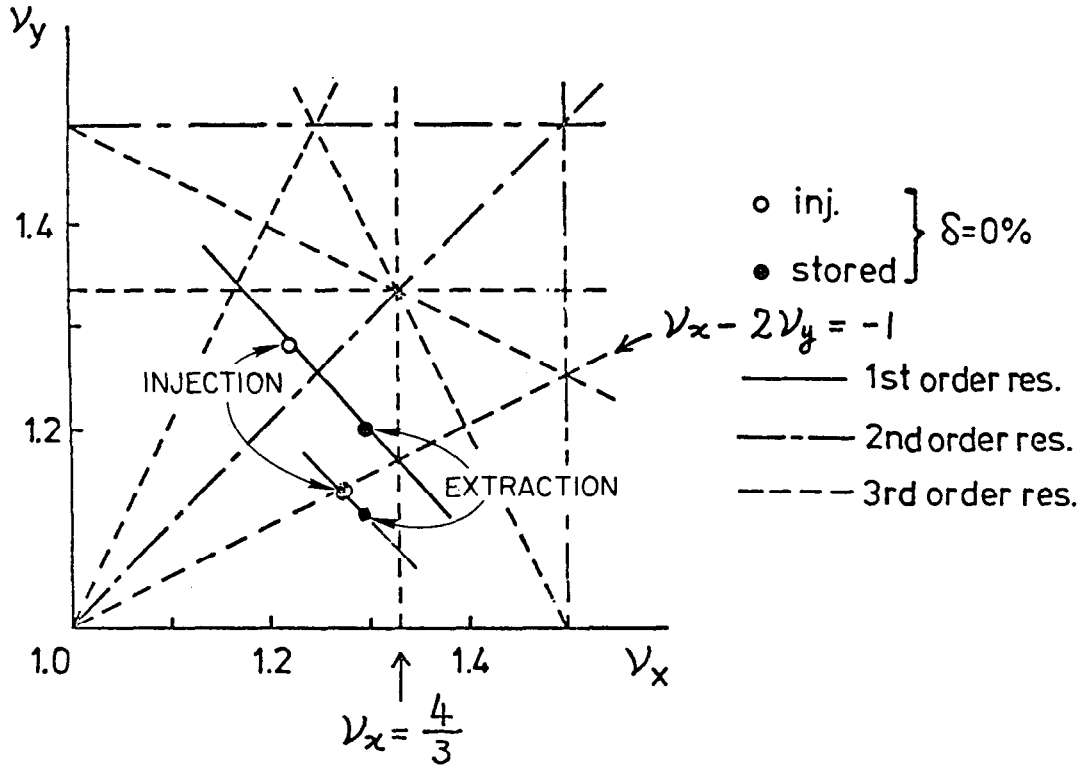

Figure 6e. SSTR betatron tune diagram showing two working injection-extraction lines.

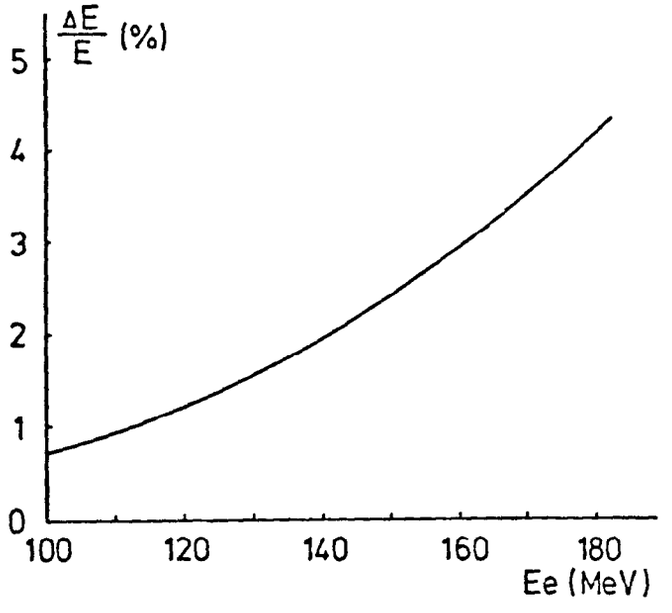

Figure 6f. Energy loss due to synchrotron radiation.

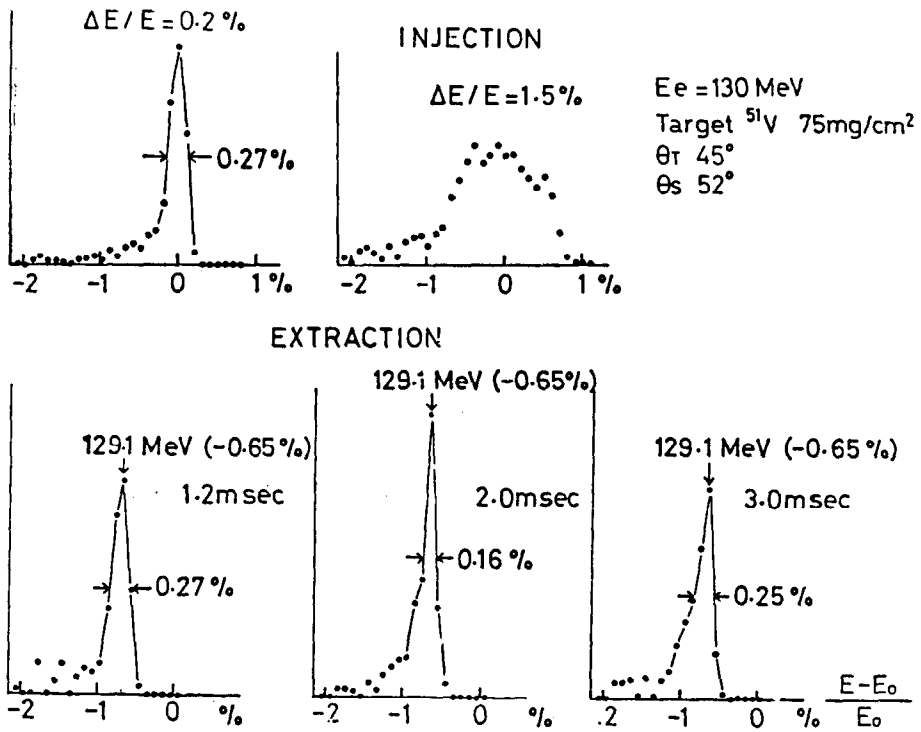

Figure 6g. Energy spectra of injected and extracted beams in SSTR. The extracted beams are measured at different sequential moments.

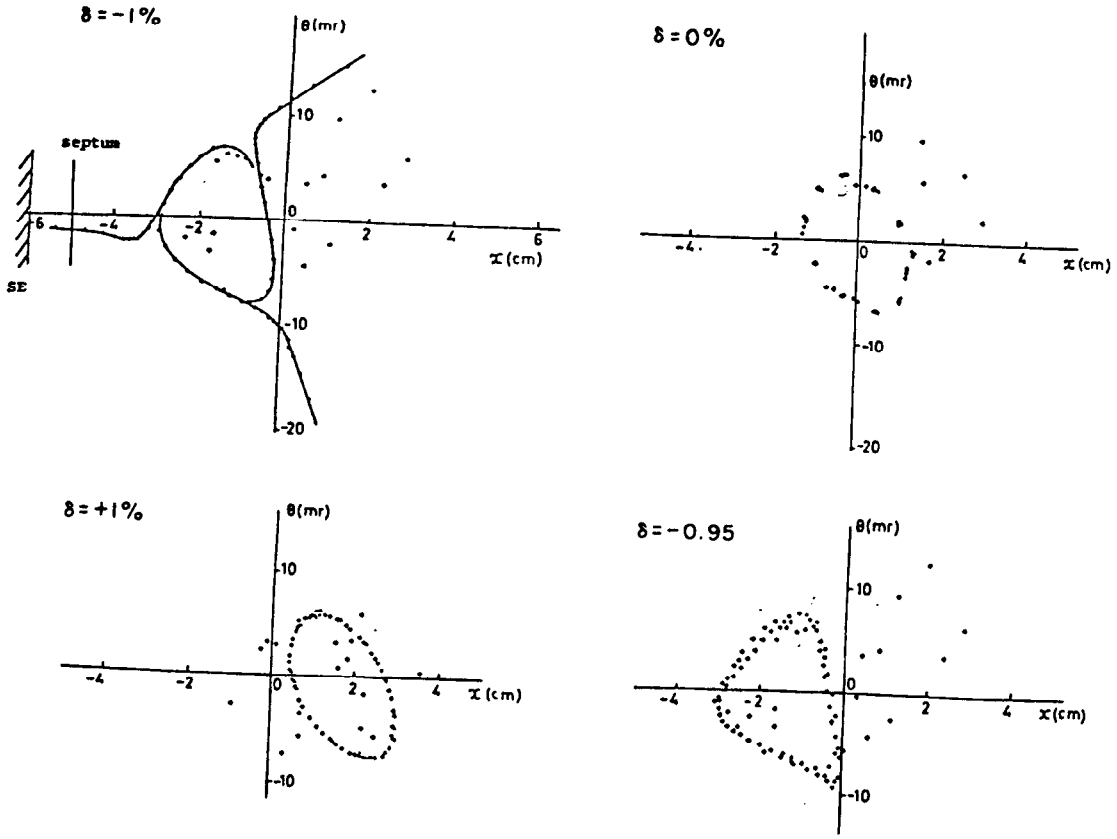

Figure 6h. Movement of a beam in horizontal phase space at end of M1 magnet at different energies.

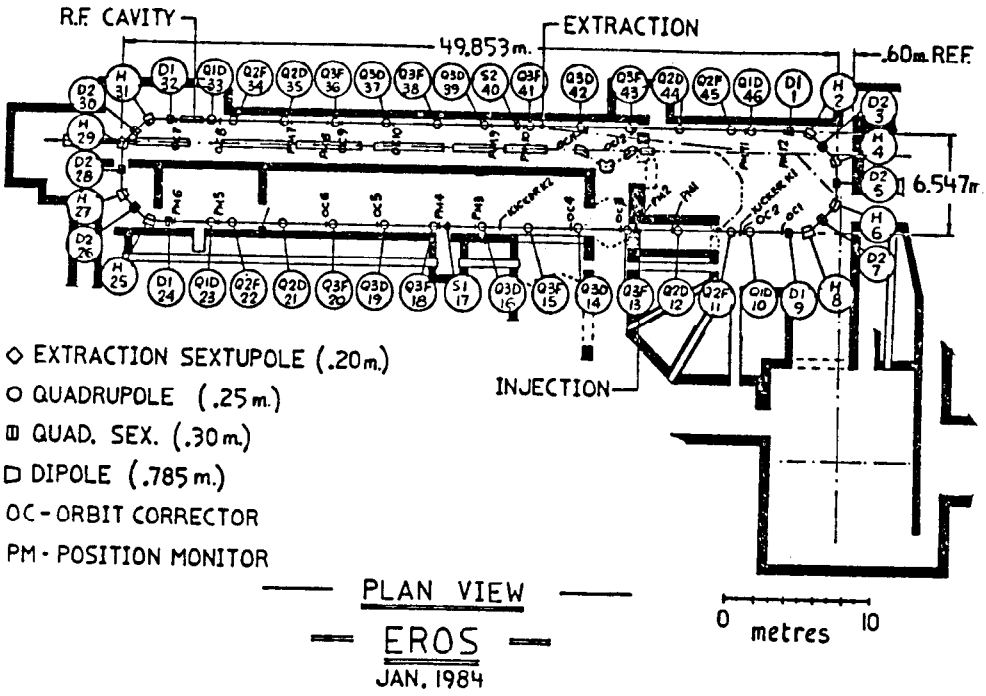

Figure 7. Layout of SAL (Saskatoon) linac and EROS stretcher.

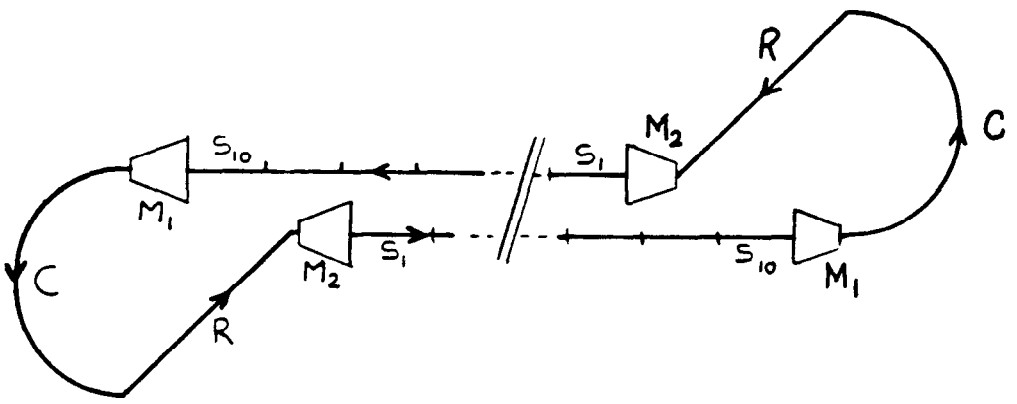

Figure 8a. Layout of NIKHEF stretcher. Note four distinguishable building blocks:

a. curved sections C
b. magnifiers M
c. return sections R
d. straight cells S_i $(i = 1 \rightarrow 10)$

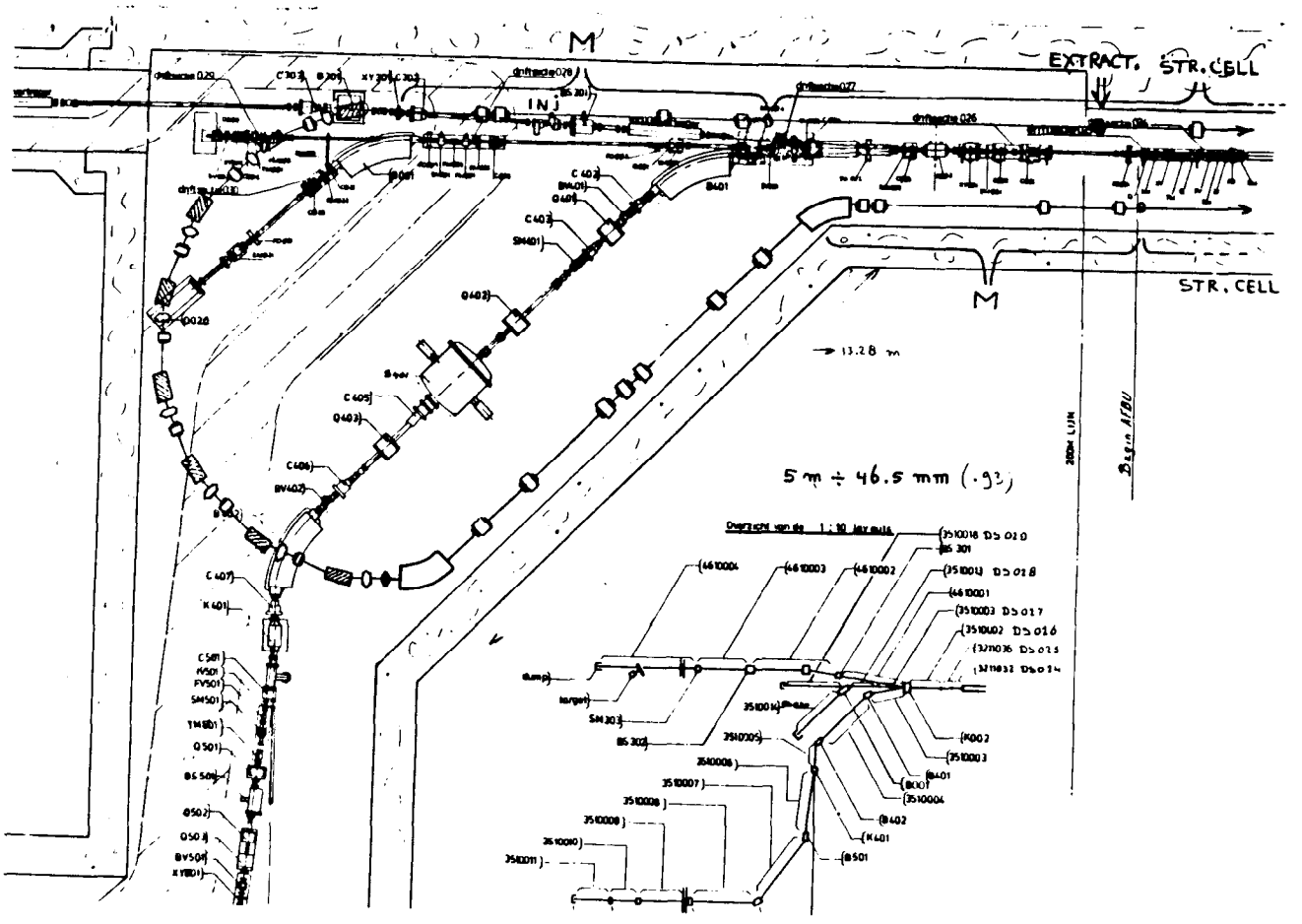

Figure 8b. Actual layout of one end-loop of NIKHEF stretcher.

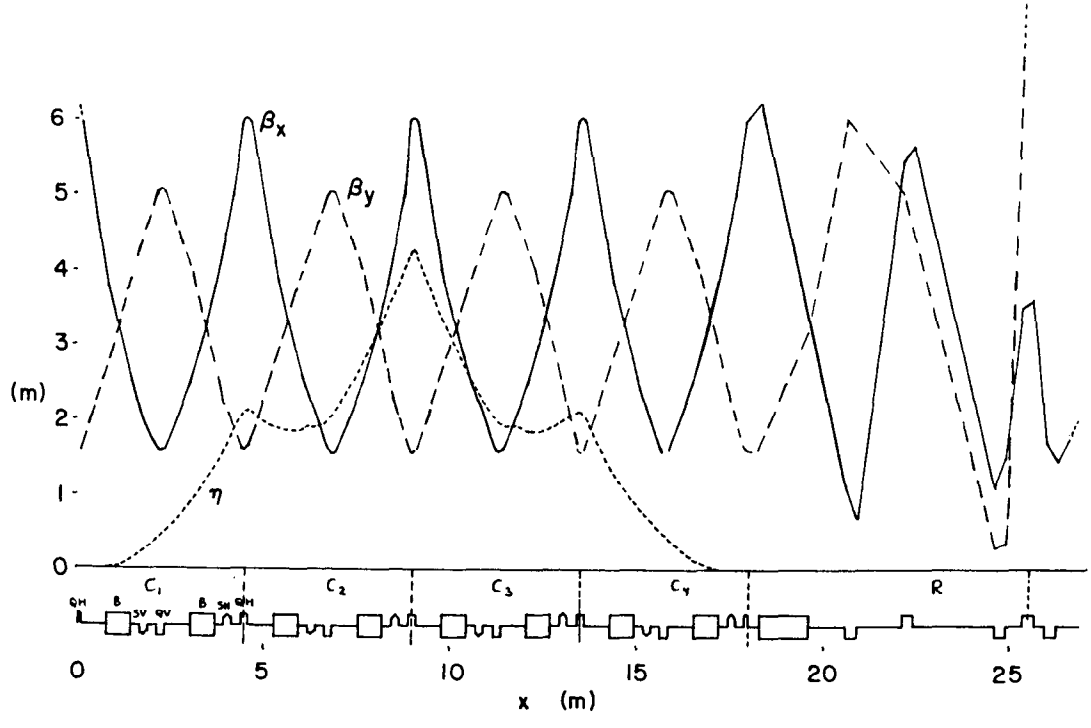

Figure 8c. η and β functions in curved section and first half of return section in NIKHEF stretcher.

funding is not yet determined. Note from the information in the fourth column and Figs. 9 that the ring is larger than some of its neighbors, partially to accommodate wigglers and other equipment. It will be operable up to at least 3.5 GeV. Two RF systems (500 MHz and 199.1 MHz) are being planned but neither will be used in the stretcher mode (300-1100 MeV). The extraction will be of the monochromatic type, making use of an injected energy spectrum of adjustable width as a function of energy. The Energy Compression System (ECS) together with the linac injector is being designed to produce spectra in the range $0.035 \rightarrow 2.23\%$.

The SACLAY project[14] in the fifth column and Figs. 10 is under active design. Funding is hoped for 1985. The existing ALS linac will undergo several major modifications. The present accelerator sections will most probably be reused but the klystrons, modulators, focussing and injector will be replaced to produce a low duty factor, higher energy, higher peak current machine. A beam recirculation system to boost the linac energy to 2 GeV might be added later. The stretcher will be entirely new. It will use a $\sim$ 600 MHz RF system to be synchronized with a sub-harmonic buncher of the same frequency in the linac injector. This frequency has been chosen to be an odd sub-harmonic of the fundamental ($\sim$ 3000 MHz) in the linac. The proposed method of extraction is of the 1/2 resonant achromatic type.

The Tohoku University STR project,[15] shown in the sixth column and in Figs. 11, is in an advanced stage of design but it has not yet been funded. The project will consist of an entirely new linac and stretcher ring. To reach the ultimate energy of 3.3 GeV, the linac will require new high power klystrons (up to 40 MW peak) and a one-turn recirculation system. Because of the high peak current in the linac, special precautions are being taken to reduce the risk of beam breakup in the disk-loaded waveguide accelerator structure. Each section will start with a slightly different iris diameter (2a) and continue with a continuously decreasing linear taper in this dimension. The goal is to make the amplification of the TM_{11} deflecting mode as incoherent and as low as possible. The recirculation loop will be equipped with an adjustable path length control (PCS) to adjust the phase of the recirculating beam on its second pass. The stretcher will have an RF system of fairly low frequency (476 MHz) and will use a 1/2 resonance achromatic extraction system. In addition to the Nuclear Physics program, this installation will also be used for the generation of synchrotron radiation, and the linac beam will be used directly for neutron generation and spectroscopy.

Finally, the SURA project[16] is shown in the last column of Table 1 and in Figs. 12. In its first stage, it is supposed to reach 4 GeV but it must be expandable to 6 GeV at a later time. The project has been approved by the U.S. Department of Energy and is expected to receive its major construction funds starting in October 1985, with a completion schedule

of five years. At the present time the linac design assumes 36 klystrons and sections and a recirculation system for two passes of $\sim$ 2 GeV each. An alternate design with 60 klystrons and 120 sections would achieve the same total energy of 4 GeV without recirculation. This scheme would result in a shorter RF pulse length (2 μsec instead of 3.2 μsec), thereby reducing the power demands placed on the klystrons, modulators, cooling systems, etc. It would also simplify the focusing and operation of the linac. On the other hand, it would lengthen the linac and the buildings housing it from 160 m to about 450 m, increasing its initial cost by \$15 to 20 M. The proposed schemes for energy compression, ring injection, extraction and RF manipulation of the beam in the ring are all illustrated in the figures. The high power RF system is only turned on for a short time after injection to rotate the beam in longitudinal phase space, thereby producing a longer bunch length in exchange of a reduced energy spread. The lower power RF system, which stays on continuously, then simply compensates for the synchrotron radiation loss. The preferred extraction system is based on the 1/2 resonance, achromatic method. The results of computer simulations for both 1/3 and 1/2 resonance schemes are shown. The size of the ring is chosen so that an expansion to 6 GeV could be obtained later without difficulty.

Special Topics

In this paper, a number of complex topics have been covered only superficially or not at all. These include phase space dilution, beam loading, beam breakup in the linac, energy compression in the ECS, injection, instabilities and extraction in the stretcher ring, and the overall subject of polarized beams. Some of these topics will be treated in greater detail during the oral presentations of the material, to the extent permitted by time.

Acknowledgements

The author wishes to acknowledge the help of many colleagues who supplied reports, references and information useful for the preparation of this paper and the lectures derived from it. In particular, he would like to thank M. Oyamada (Tohoku University), R. V. Servranckx (SAL), S. Penner (NBS), T. I. Smith (HEPL), B. E. Norum and R. C. York (University of Virginia), and B. Aune (SACLAY).

References

1. Penner, Samuel, *CW Electron Accelerators for Nuclear Physics*, Proceedings of the 1981 Particle Accelerator Conference, Accelerator Engineering and Technology, IEEE Transactions on Nuclear Science, Vol. **NS-28**, 2067 (1981).

2. Axel, P., L. S. Cardman, H. D. Graef, A. O. Hanson, R. A. Hoffswell, D. Jamnik, D. C. Sutton, R. H. Taylor and L. M. Young, *Operating Experience with MUSL-2*, IEEE Transactions on Nuclear Science, Vol. **NS-26**, 3143 (1979).

3. Herminghaus, H., B. Dreher, H. Futeneuer, K. H. Kaiser, M. Kelliher, R. Klein, H. J. Kreidel, M. Loch, U. Ludwig-Mertin, K. Merle, H. Schoeler, R. Schulze, P. Semmel, G. Stephan, *Status Report on the Normal Conducting CW Racetrack Microtron Cascade "Mami"*, Proceedings of the 1983 Particle Accelerator Conference, Accelerator Engineering and Technology, IEEE Transactions on Nuclear Science, Vol. **NS-30**, 3274 (1983).

4. Penner, S. *The NBS Proposal for a One GeV CW Racetrack Microtron Facility*, Proceedings of the 1983 Particle Accelerator Conference, Accelerator Engineering and Technology, IEEE Transactions on Nuclear Science, Vol. **NS-30**, 3279 (1983).

5. Kustom, R. L., *GEM, ANL 4-GeV CW Electron Microtron Design*, Proceedings of the 1983 Particle Accelerator Conference, Accelerator Engineering and Technology, IEEE Transactions on Nuclear Science, Vol. **NS-30**, 3286 (1983).

6. Lyneis, C. M., M. S. McAshan, R. E. Rand, H. A. Schwettman, T. I. Smith, and J. P. Turneaure, *Unique Beam Properties of the Stanford 800 MeV Superconducting Recyclotron*, Special Issue, 1981 Particle Accelerator Conference, Accelerator Engineering and Technology, IEEE Transactions on Nuclear Science, Vol. **NS-28**, No. 3, 3445 (1981).

7. Eriksson, Mikael, *The Acccelerator System Max*, Nuclear Instruments and Methods, Vol. **196**, 331 (1982).

8. Husmann, D., *ELSA, A Stretcher and Post Accelerator for the Bonn 2.5-GeV Electron Synchrotron*, Proceedings of the 1983 Particle Accelerator Conference, Accelerator Engineering and Technology, IEEE Transactions on Nuclear Science, Vol. **NS-30**, 3252 (1983).

9. See for example, *The Stanford Two-Mile Accelerator*, (R. B. Neal, General Editor) New York: W. A. Benjamin, Inc. (1968).

10. Tamae, T., M. Sugawara, O. Konno, T. Sasanuma, T. Tanaka, M. Muto, K. Yoshida, M. Hirooka, Y. Shibazaki, K. Yamada, T. Terasawa, M. Urasawa, T. Ichinohe, S. Takahashi, H. Miyase, Y. Kawazoe, S. Yamamoto, and Y. Torizuka, *150-MeV*

Pulse Stretcher of Tohoku University, Proceedings of the 1983 Particle Accelerator Conference, Accelerator Engineering and Technology, IEEE Transactions on Nuclear Science, Vol. **NS-30**, 3235 (1983).

11. Bergstrom, J. C., H. S. Caplan and R. V. Servranckx, *SORE - A Pulse Stretcher for the Saskatchewan 300-MeV Linac*, Proceedings of the 1983 Particle Accelerator Conference, Accelerator Engineering and Technology, IEEE Transactions on Nuclear Science, Vol. **NS-30**, 3226 (1983).

12. Maas, R., notes on *The NIKHEF Stretcher - the first ideas*, NIKHEF, Amsterdam, The Netherlands, preprint 830504/RM.

13. *Progetto ALFA TRE*, Instituto Nazionale di Fisica Nucleare, Laboratori Nazionali di Frascati, **LNF-81/18** (1981).

14. Aune, B., C. Grunberg, M. Jablonka, F. Koechlin, J. Magne, A. Mosnier, B. Phung and F. Netter, *ALS II: The Saclay Proposal for a 2-GeV, CW Electron Facility*, Proceedings of the 1983 Particle Accelerator Conference, Accelerator Engineering and Technology, IEEE Transactions on Nuclear Science, Vol. **NS-30**, 3296 (1983).

15. Saito, T., *Status Report, Tohoku Linac and Stretcher*, presented at the Magnetic Spectrometer Workshop, Williamsburg, Virginia, October 1983.

16. *Proposal for a National Electron Accelerator Laboratory*, Southeastern Universities Research Association (1982).

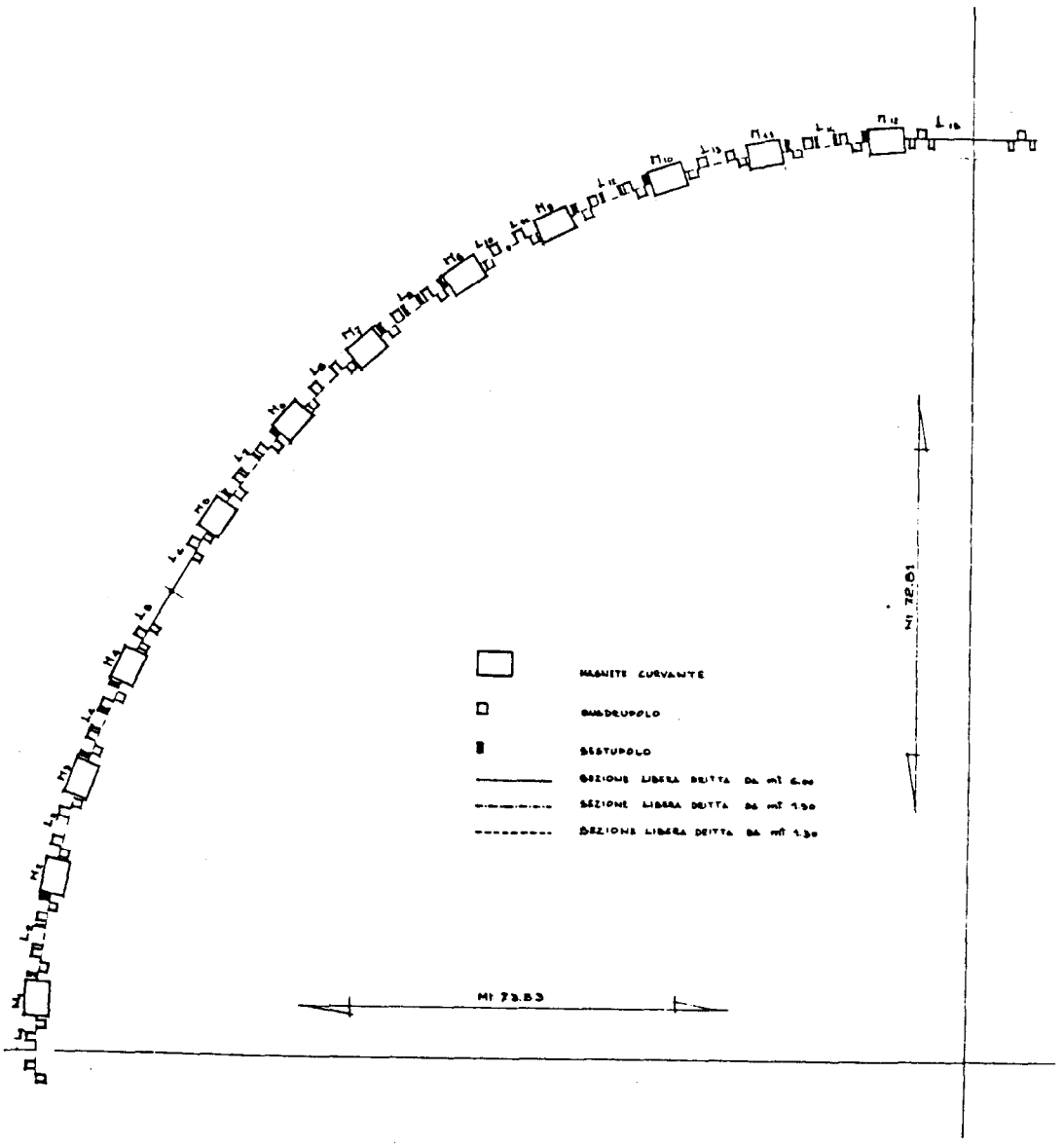

Figure 9a. Layout of one-fourth of Frascati stretcher ring.

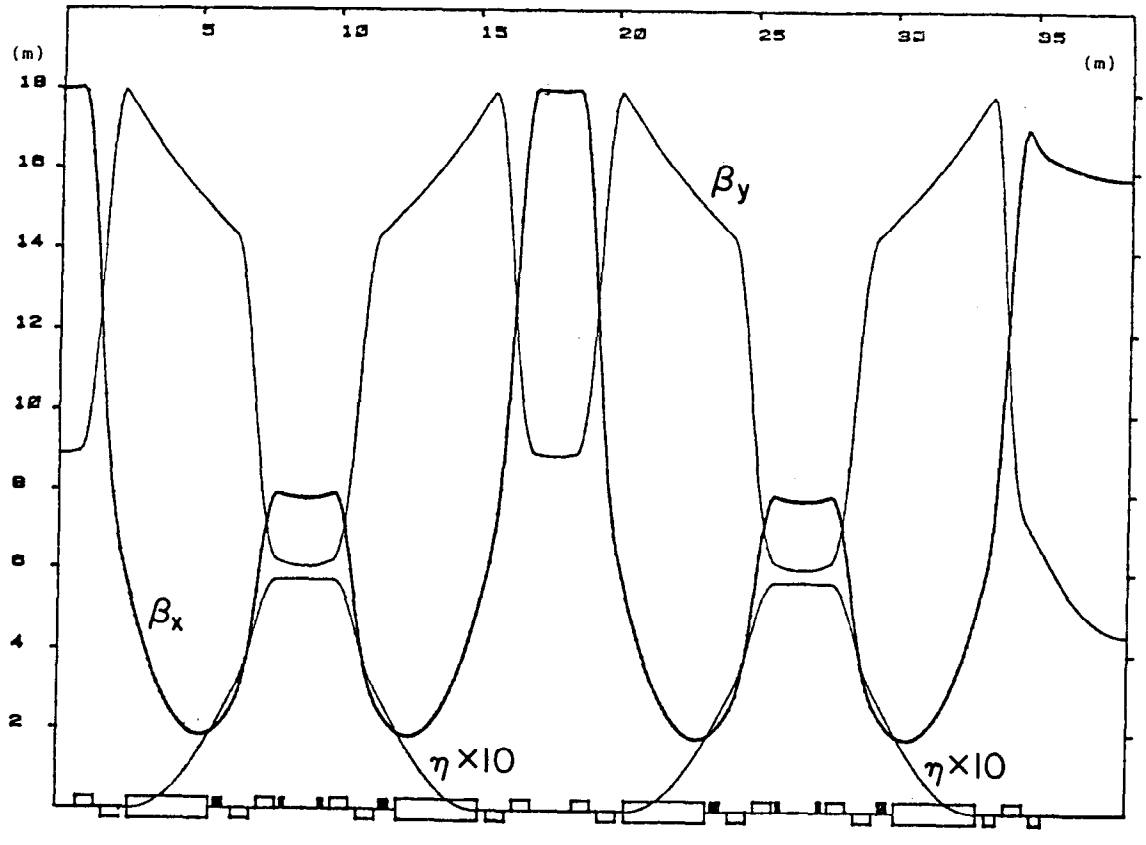

Figure 9b. η and β functions in one-half period in Frascati stretcher.

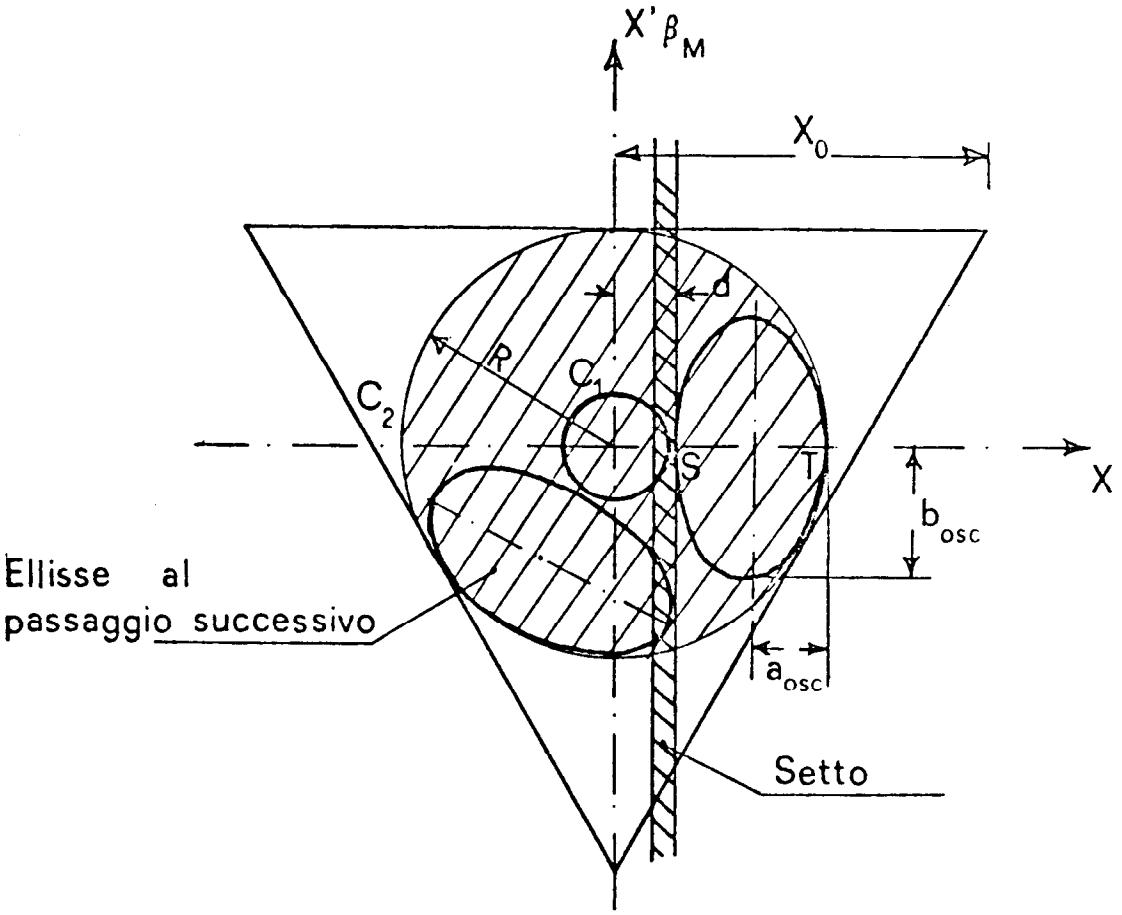

Figure 9c. Two-turn injection into stretcher phase space.

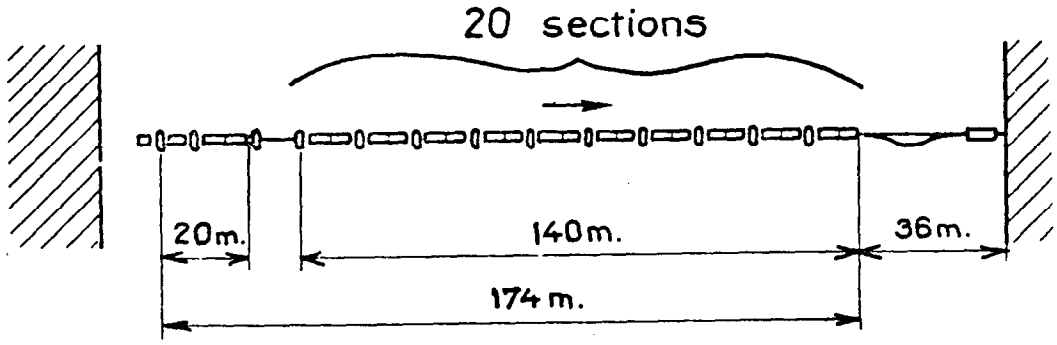

Figure 10a. Layout of transformed SACLAY linac.

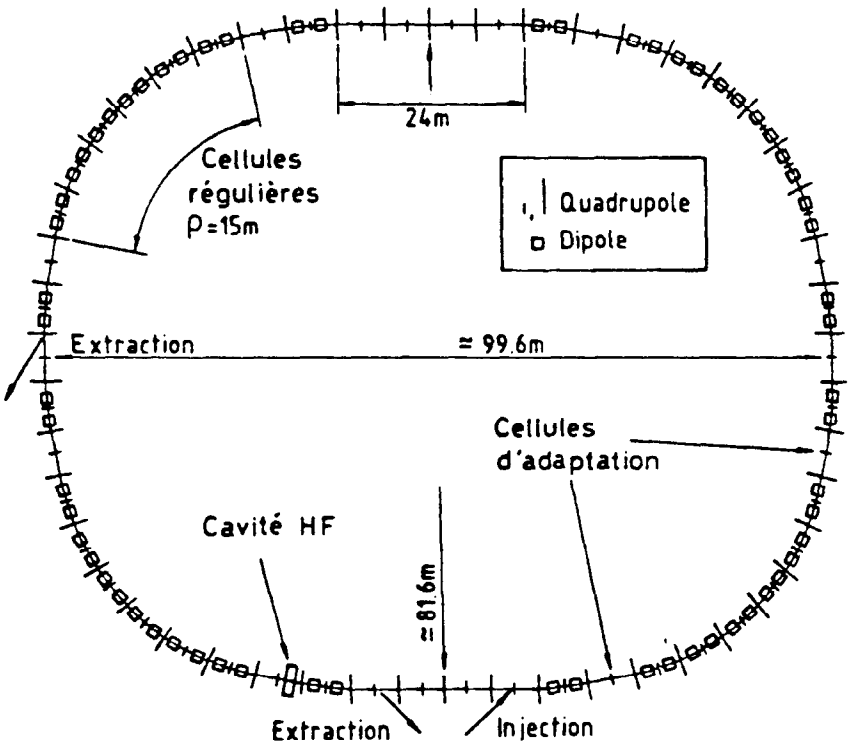

Figure 10b. Configuration of SACLAY stretcher ring.

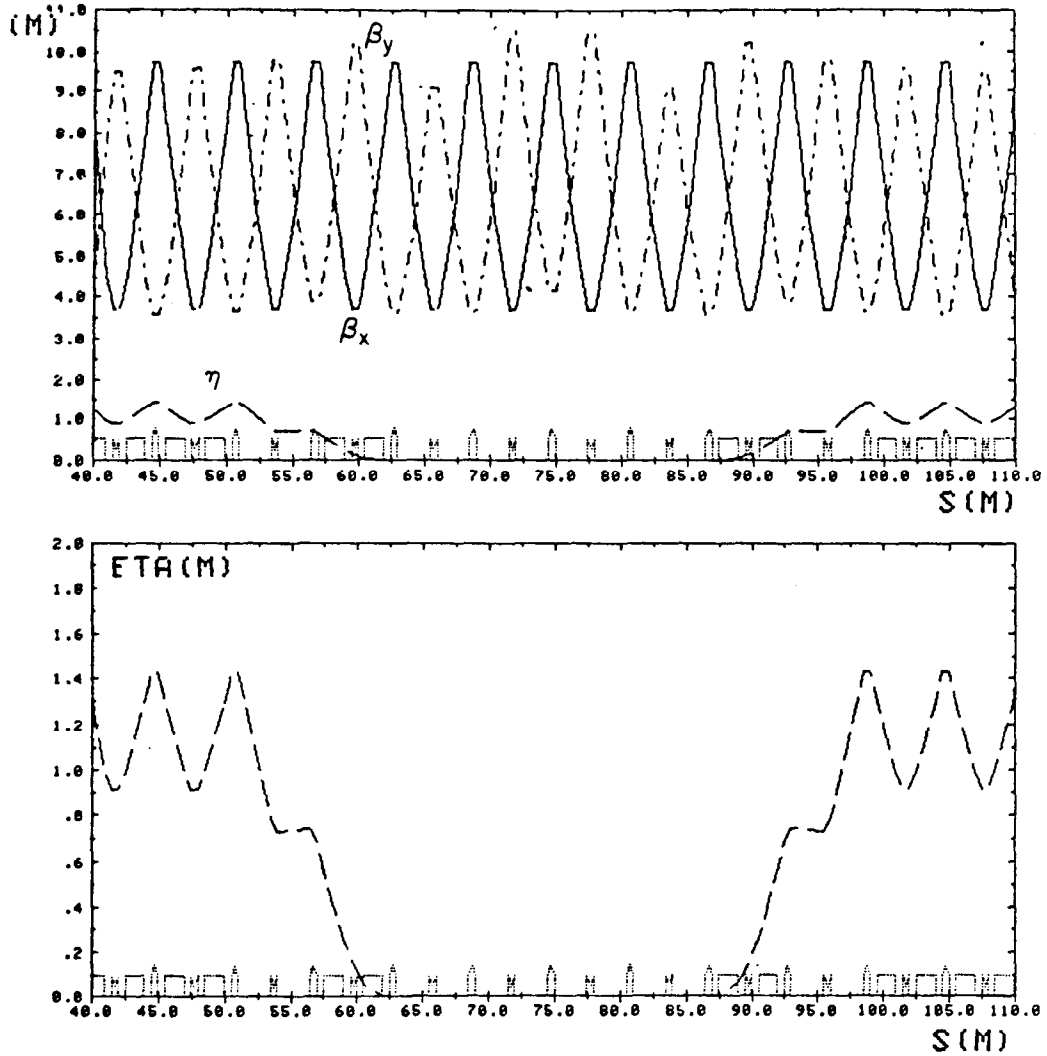

Figure 10c. β and η functions in SACLAY stretcher.

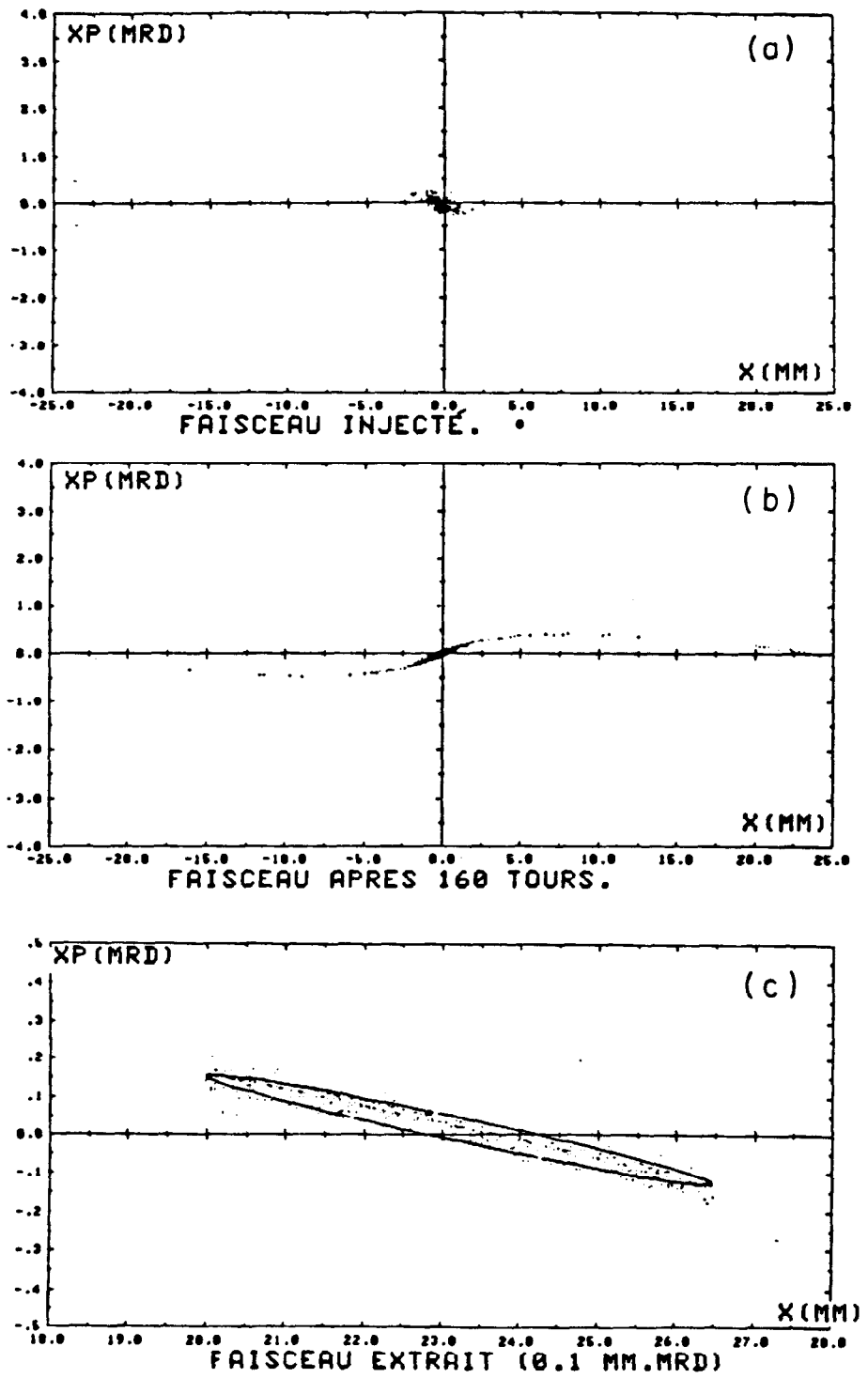

Figure 10d. Scenario of one-half resonance beam extraction in SACLAY stretchers.

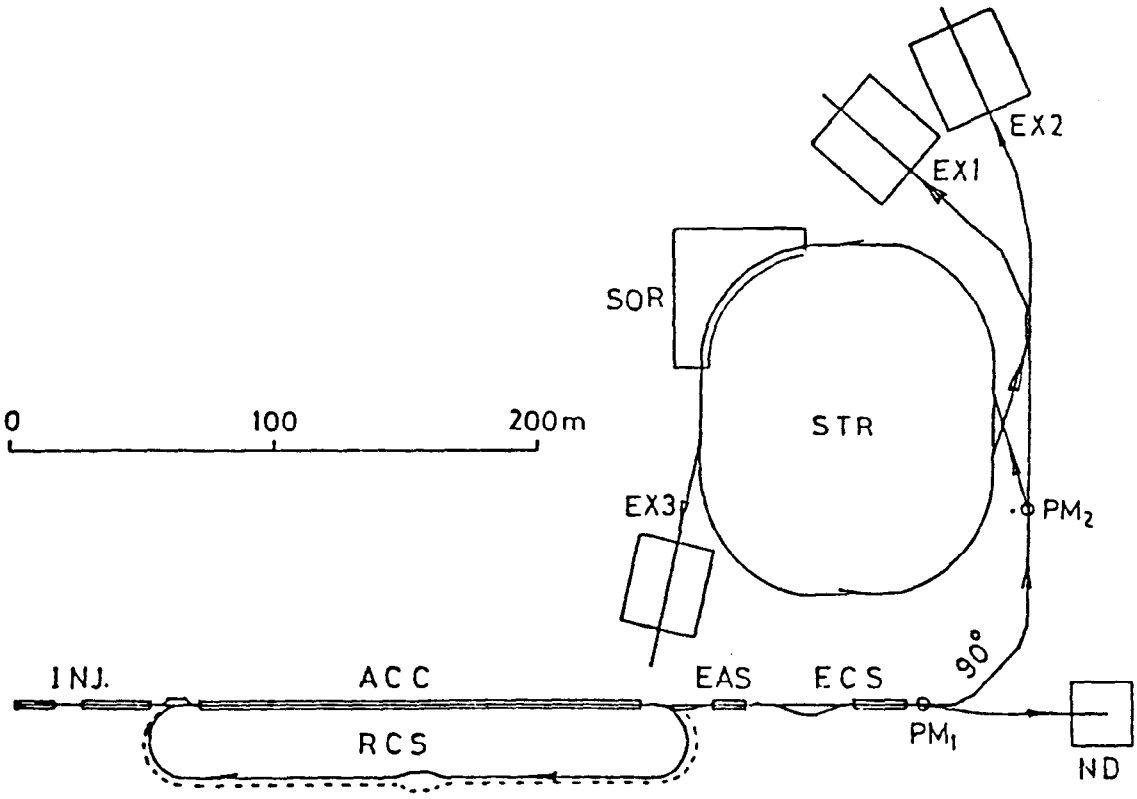

Figure 11a. Proposed Tohoku electron accelerator facility.

INJ — injector

ACC — main accelerator

RCS — recirculation system

EAS — energy adjusting system

ECS — energy compression system (dotted line: phase II)

$PM_{1,2}$ — pulse magents

ND — neutron diffraction hall

STR — pulse stretcher ring

$EX_{1,2,3}$ — nuclear experimental halls

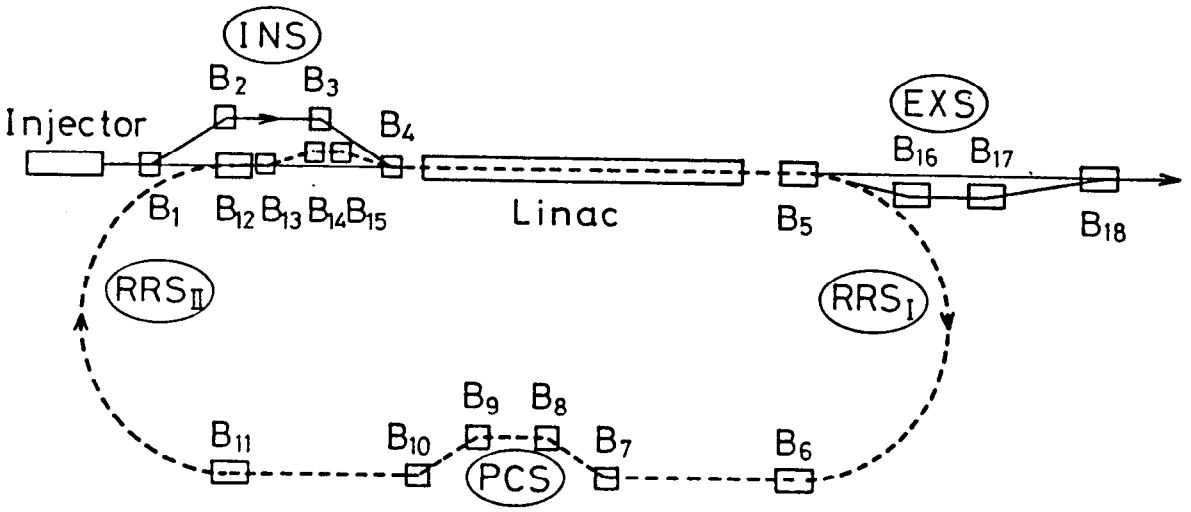

Figure 11b. Proposed Tohoku injector, linac and recirculation system with Phase Control System (PCS).

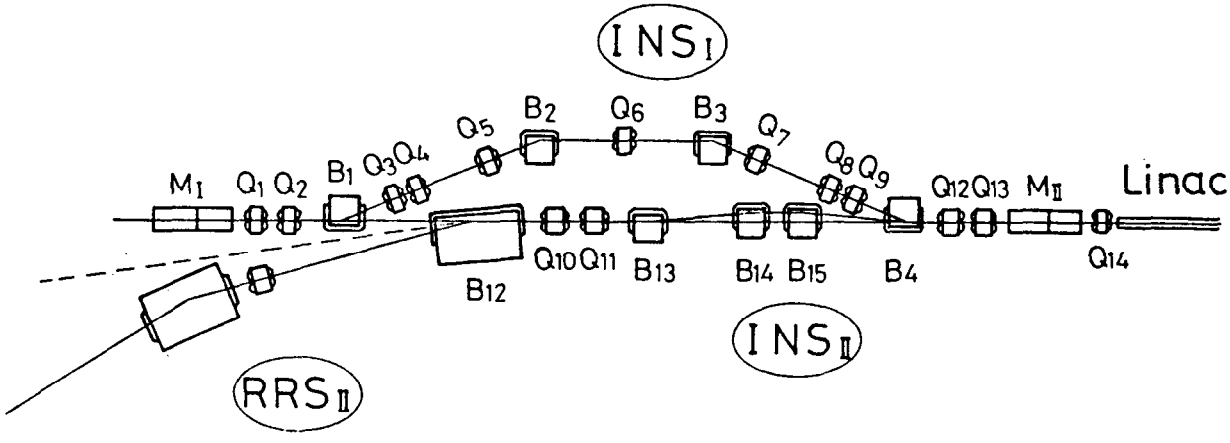

Figure 11c. Details of injector and recirculated beam insertion into linac.

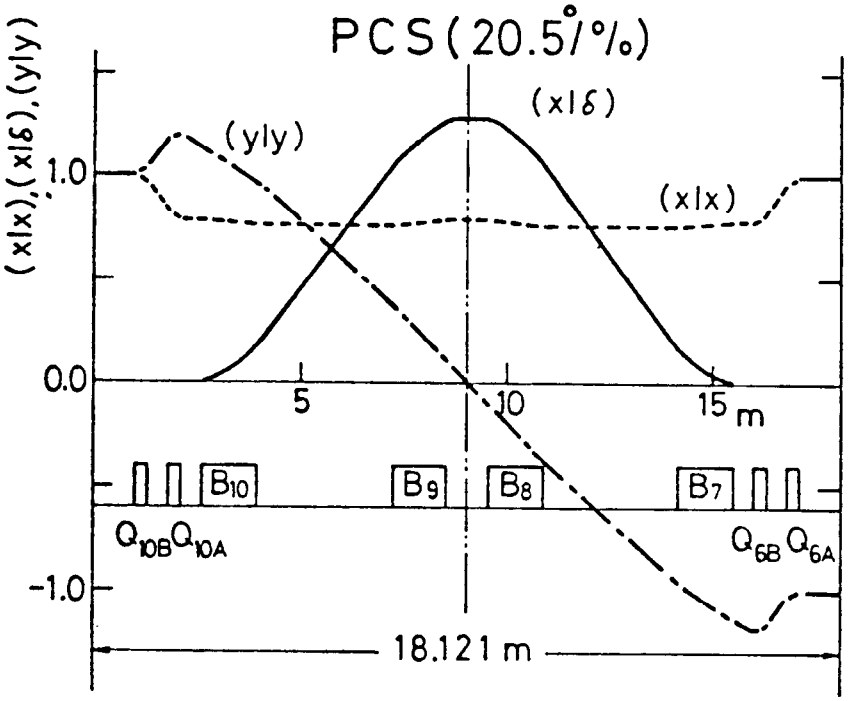

Figure 11d. Details of Phase Control System (PCS).

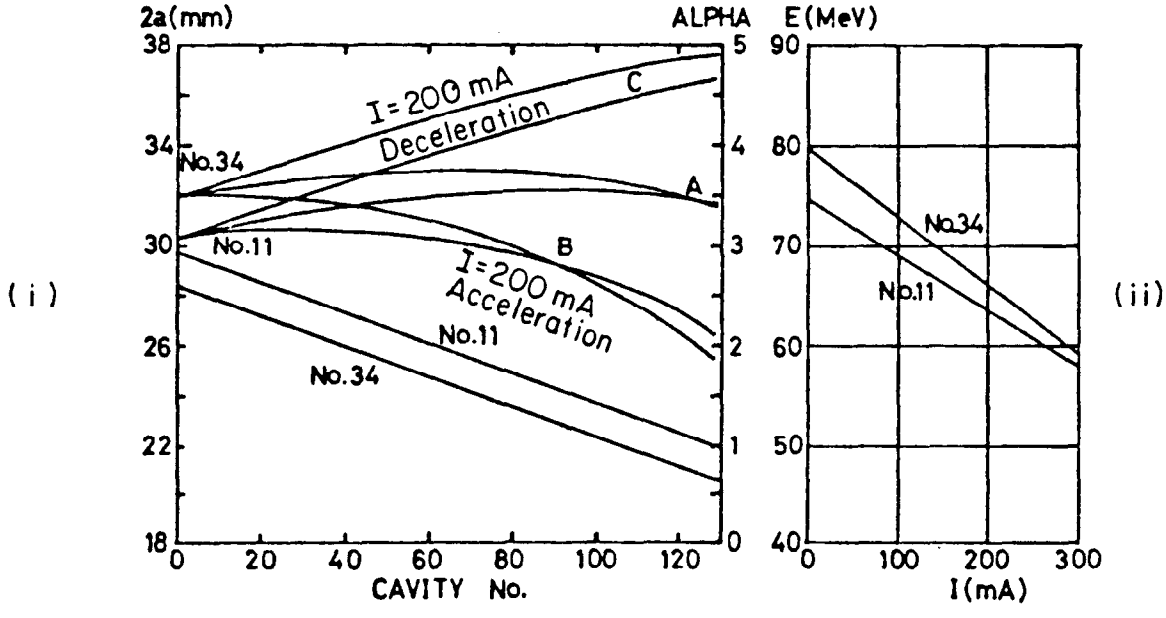

Figure 11e. Disk-loaded accelerator structure characteristics.

i) Field (α) and iris diameter (2a) versus cavity number;

ii) Energy per section versus current.

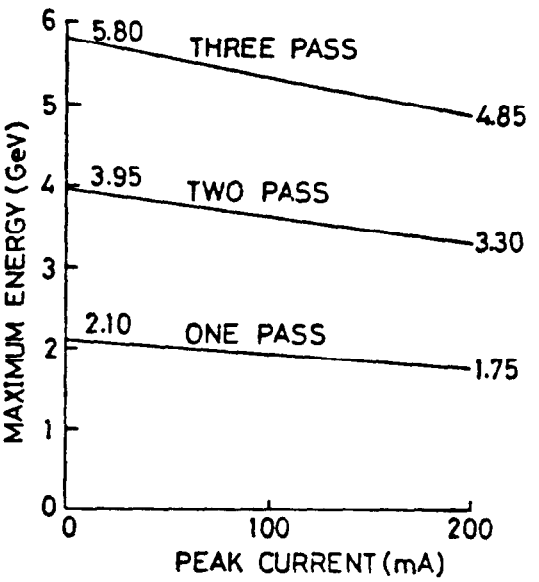

Figure 11f. Linac energy versus peak current as a function of number of passes.

PEAK POWER OUTPUT OF KLYSTRON = 40 MW

ATTENUATION OF FEEDING WAVE GUIDE = 0.62 dB

No.	iris diameter		no-load energy	beam loading	filling time	attenuation	Remarks
	2a(0) (mm)	2a(129) (mm)	V(i=0) (MeV)	-dV/di (MeV/A)	t_f (μsec)	τ (neper)	
1	32.40	24.66	63.82	36.48	0.57	0.38	ECS
2	32.34	24.60	64.09	36.87	0.57	0.38	
3	32.28	24.54	64.36	37.27	0.57	0.38	EFC
4	32.22	24.48	64.62	37.67	0.58	0.39	
5	32.16	24.42	64.88	38.06	0.58	0.39	Injector
6	32.10	24.36	65.15	38.46	0.59	0.39	
7	32.04	24.30	65.41	38.86	0.59	0.40	
11	29.76	22.02	74.65	55.68	0.81	0.57	
12	29.70	21.96	74.88	56.18	0.82	0.57	Main
13	29.64	21.90	75.11	56.69	0.83	0.58	Linac
14	29.58	31.84	75.34	57.19	0.84	0.58	
15	29.52	21.78	75.57	57.70	0.84	0.59	
16	29.46	21.72	75.80	58.22	0.85	0.59	Sector
17	29.40	21.66	76.03	58.74	0.86	0.60	1
18	29.34	21.60	76.26	59.26	0.87	0.61	
19	29.28	21.54	76.48	59.79	0.87	0.61	
20	29.22	21.48	76.71	60.32	0.88	0.62	Main
21	29.16	21.42	76.93	60.85	0.89	0.62	Linac
22	29.10	21.36	77.16	61.39	0.90	0.63	
23	29.04	21.30	77.38	61.93	0.91	0.63	
24	28.98	21.24	77.60	62.47	0.91	0.64	Sector
25	28.92	21.18	77.82	63.02	0.92	0.65	2
26	28.86	21.12	78.04	63.58	0.93	0.65	
27	28.80	21.06	78.26	64.14	0.94	0.66	
28	28.74	21.00	78.48	64.70	0.95	0.67	Main
29	28.68	20.94	78.70	65.27	0.96	0.67	Linac
30	28.62	20.88	78.92	65.84	0.96	0.68	
31	28.56	20.82	79.14	66.41	0.97	0.68	
32	28.50	20.76	79.35	66.99	0.98	0.69	Sector
33	28.44	20.70	79.57	67.58	0.99	0.70	3
34	28.38	20.64	79.78	68.16	1.00	0.70	

Figure 11g. Parameters of accelerator sections.

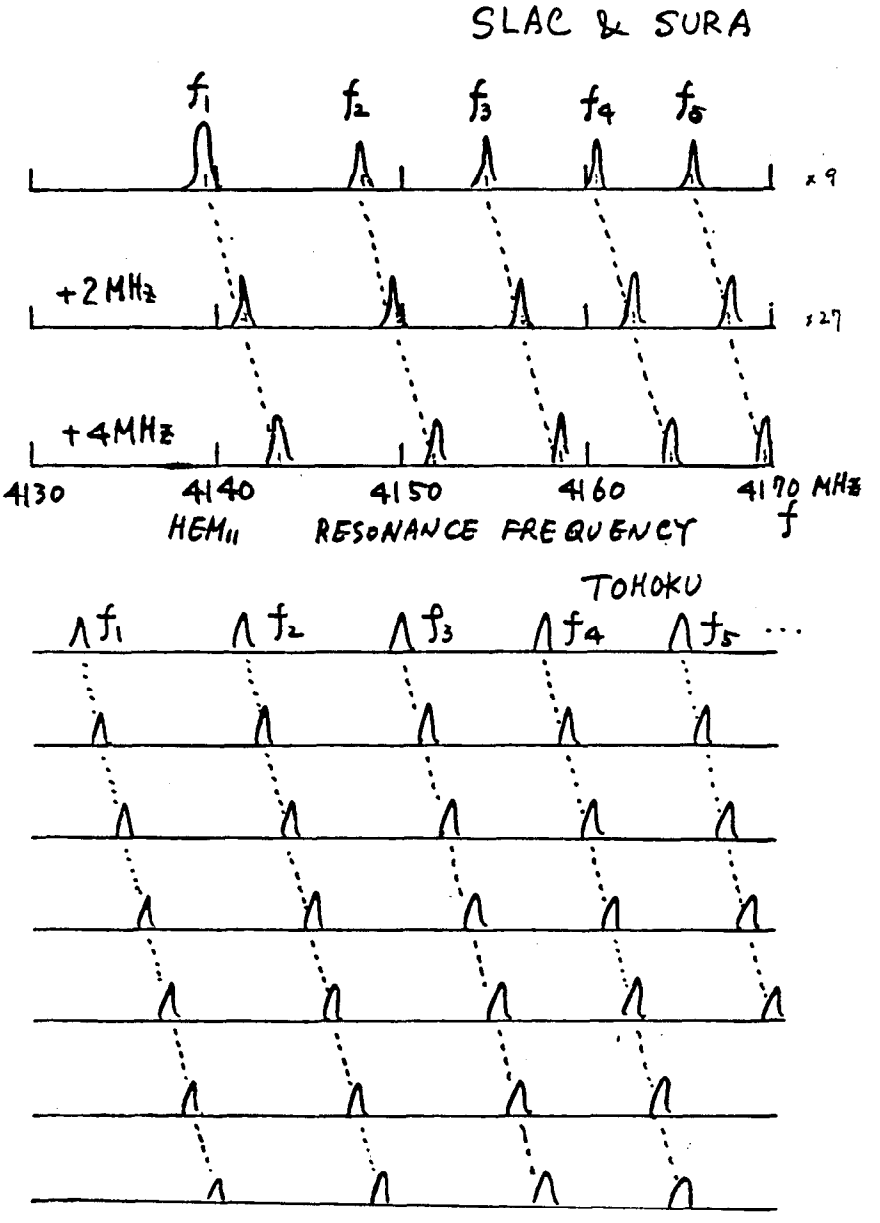

Figure 11h. Beam breakup resonances.

Parameter	Unit	PV−3030A	PV−3030B	PV−3040
Maximum				
Peak Beam Voltage	kV	270	270	315
Peak Beam Current	A	295	295	355
Peak Beam Power	MW	80	80	110
Average Beam Power	kW	40	100	130
Beam Duty	10^{-3}	0.5	1.25	1.2
Typical				
Microperveance	10^{-6} A/V$^{3/2}$	2.1	2.1	2.0
Peak Beam Voltage	kV	260	260	300
Peak Beam Current	A	280	280	330
Beam Pulse Width	μsec	5.0	4.1	4.0
RF Pulse Width	μsec	4.0	3.3	3.0
Repetition Rate	pulses/sec	100	300	300
Beam Duty	10^{-3}	0.5	1.23	1.2
RF Duty	10^{-3}	0.4	0.99	0.9
Peak Drive Power	W	400	300	300
Peak Power Output	MW	30	30	40
Average Power Output	kW	12	30	36
Efficiency	%	41	41	41
Gain	dB	49	50	51
Focusing		Permanent Magnet	Electromagnet	Electromagnet
Size (Height)	mm	1317	1317	1663
Laboratory		KEK	TOHOKU	TOHOKU

Figure 11i. Comparison of MELCO klystron specifications.

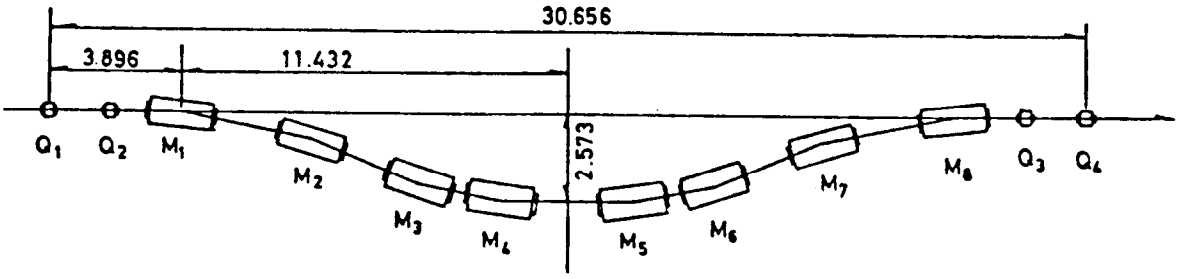

Figure 11j. Energy compression magnetic system.

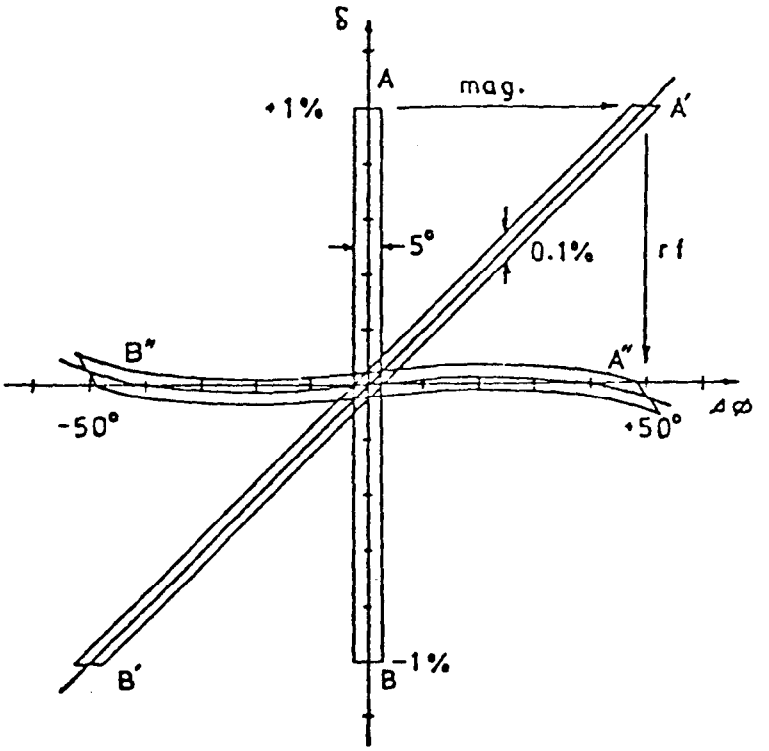

Figure 11k. Operation of Energy Compressing System (ECS).

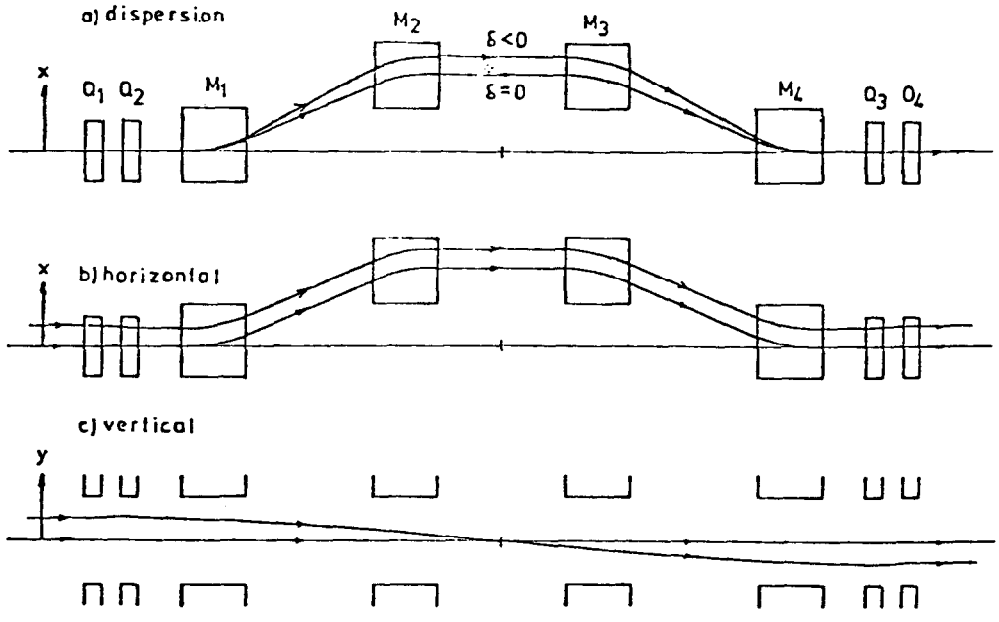

Figure 11m. Orbits in ECS magnets.

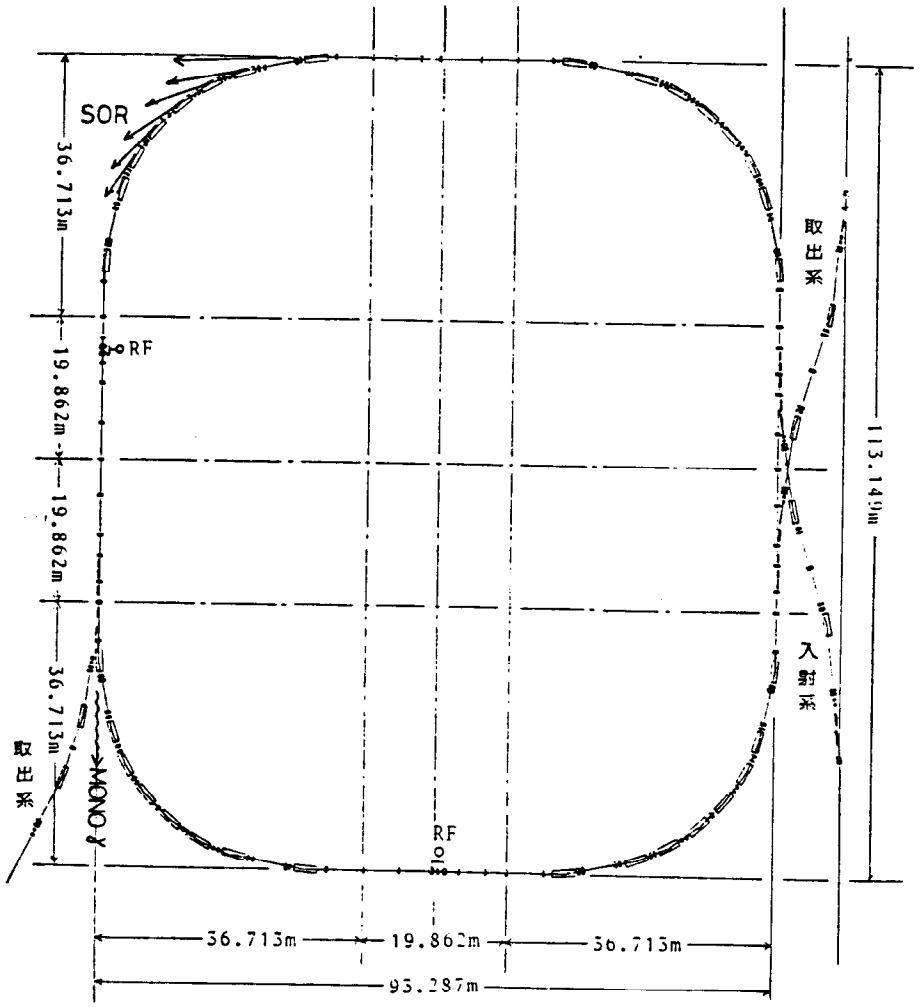

Figure 11n. Configuration of TOHOKU stretcher ring.

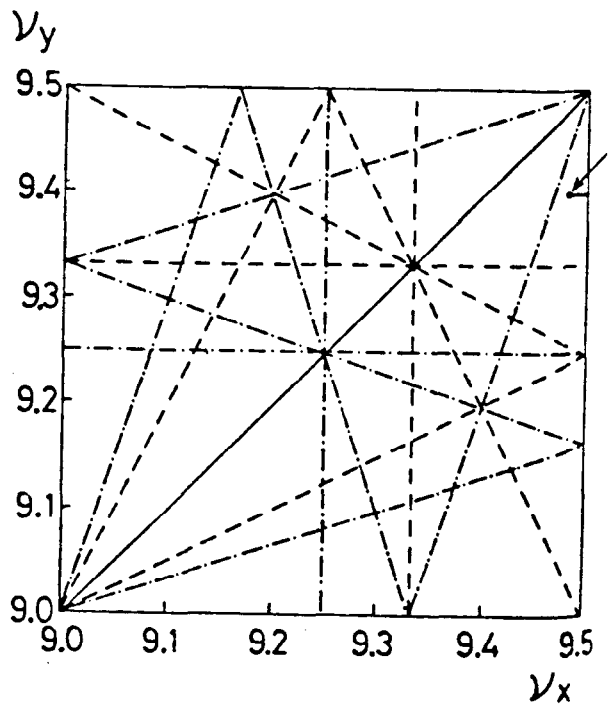

Figure 11o. Stretcher betatron tune diagram.

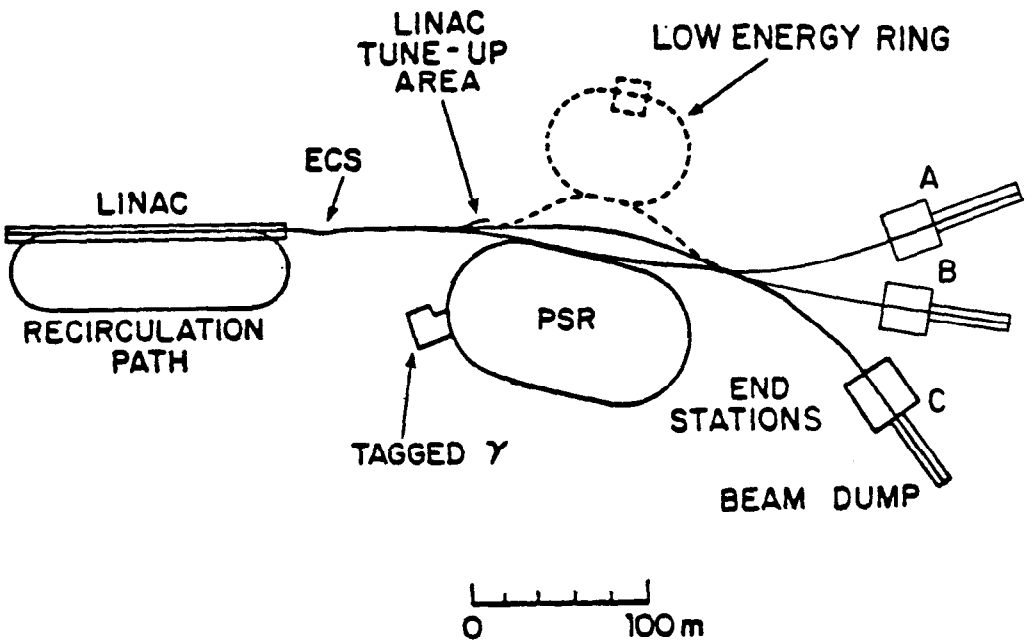

Figure 12a. SURA overall layout.

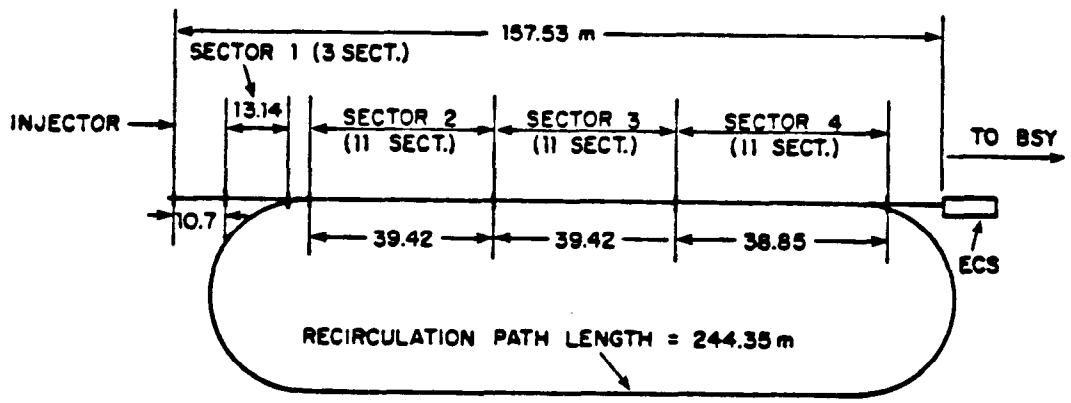

Figure 12b. SURA linac-recirculator layout.

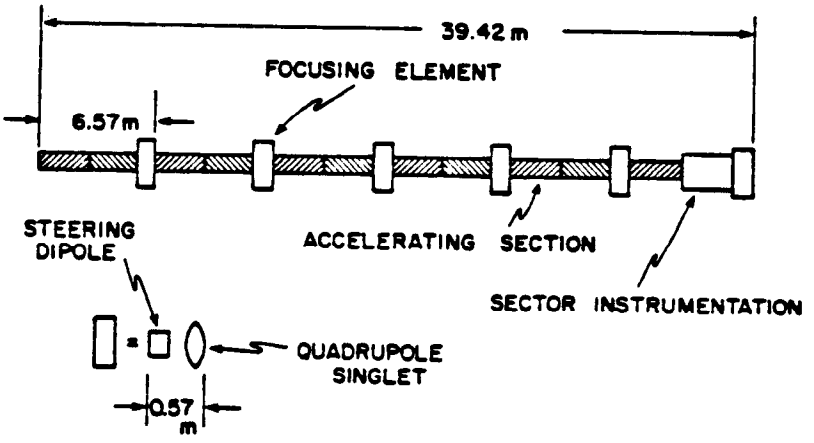

Figure 12c. Typical linac sector (Sector 2) layout.

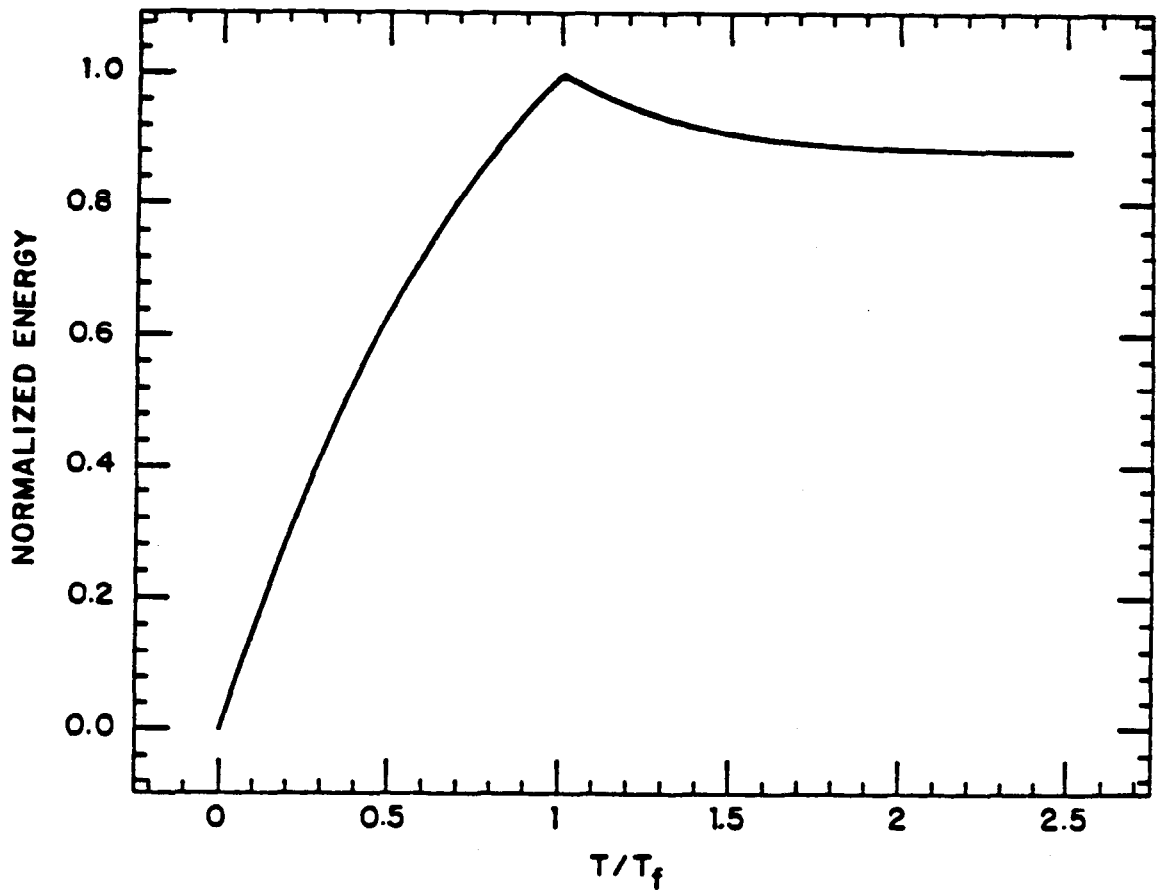

Figure 12d. Normalized, loaded, beam energy when the beam pulse is injected into the accelerator one fill time after the RF has been turned on.

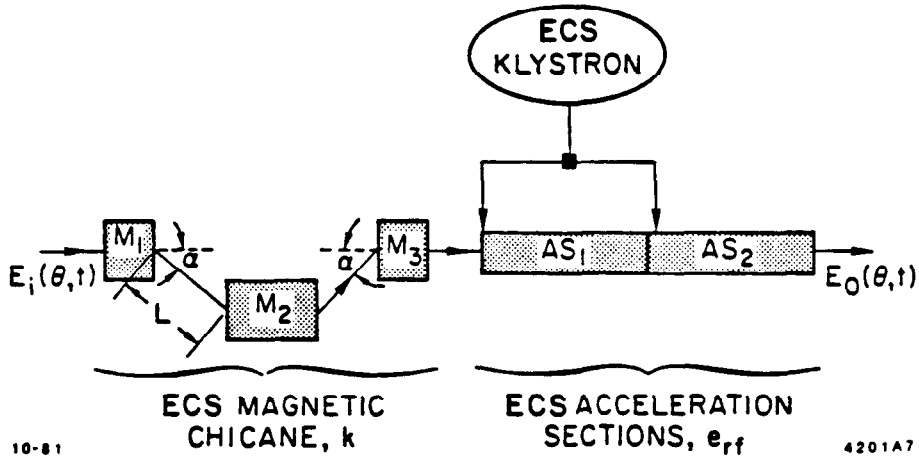

Figure 12e. SURA energy compression system.

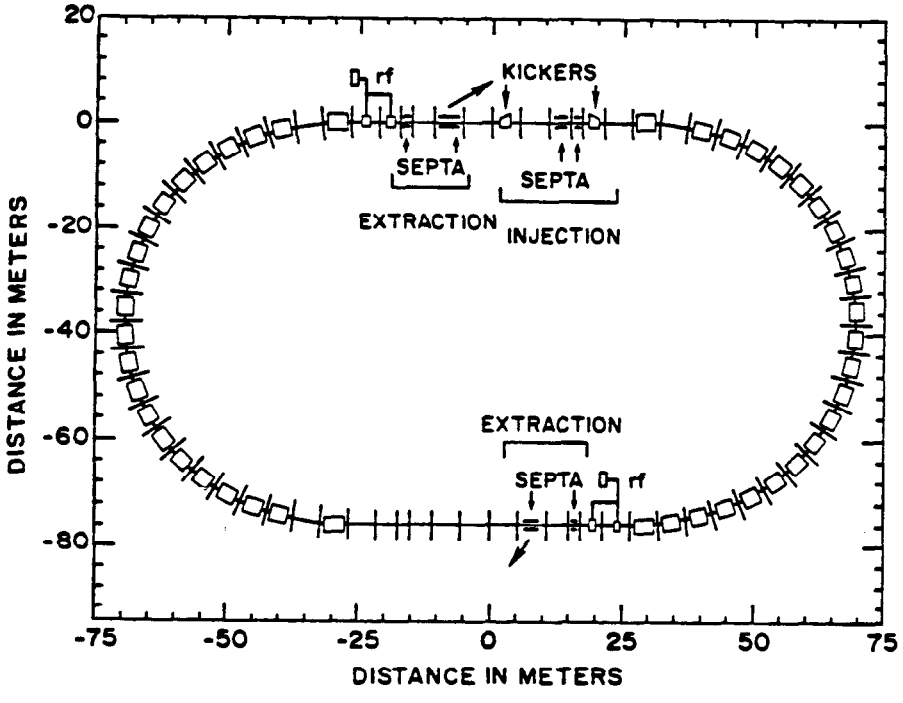

Figure 12f. SURA stretcher lattice.

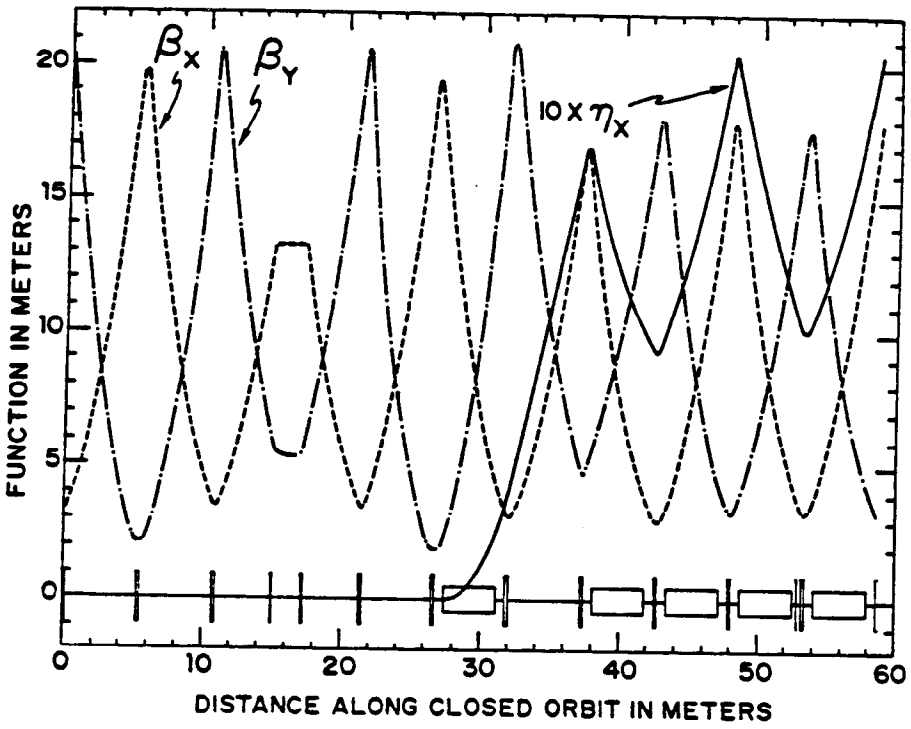

Figure 12g. β and η functions in representative cells of the SURA stretcher.

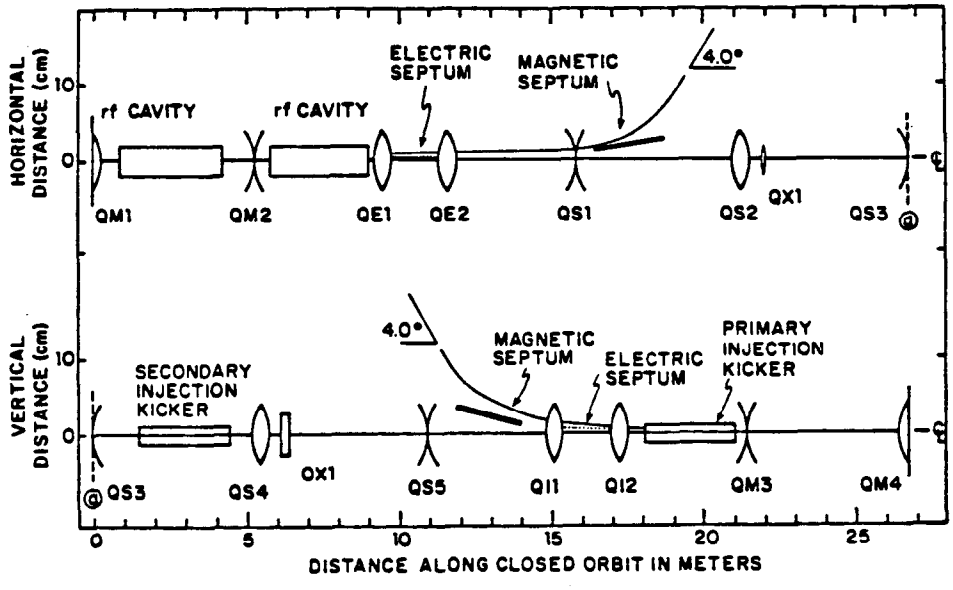

Figure 12h. Straight section layout insertion.

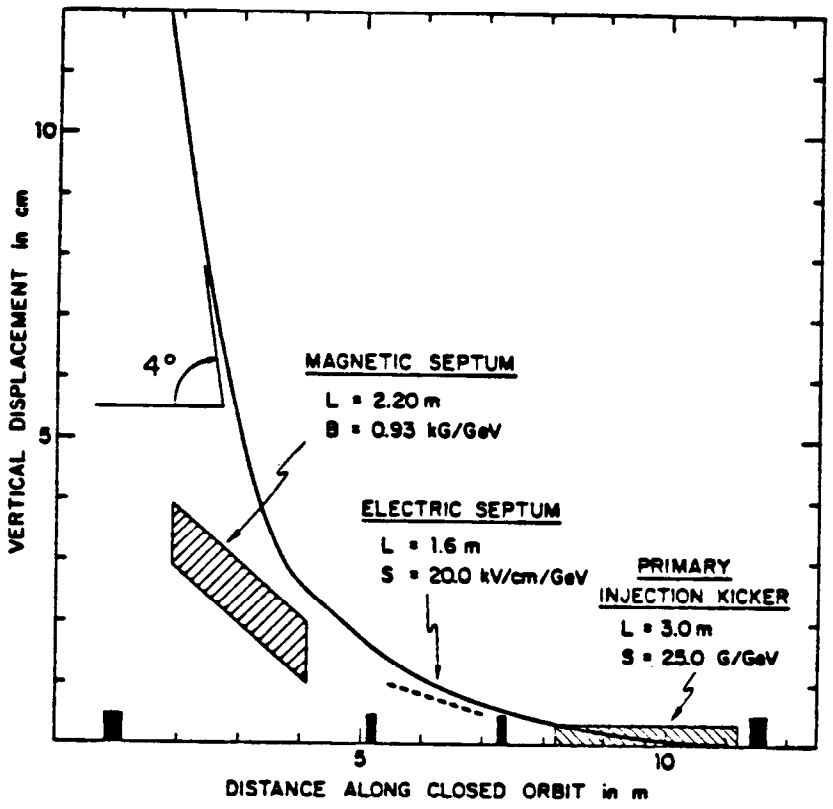

Figure 12i. Linac pulse injection into pulse stretcher.

Injection Kickers:	Primary	Secondary
Repetition Rate (H_z)	1000	1000
Rise/Fall Time (nsec)	80	80
Flat Top (μsec)	1.2	1.2
Strength (G-m/GeV)	75.0	37.5
Deflection Angle (mrad)	2.24	1.12
Electric Septum:		
Length		1.6 m
Strength		20.0 kV/cm/GeV
Septum Thickness		50.0 μm
Deflection Angle		3.2 mrad
Magnetic Septum:		
Length		2.2 m
Strength		0.93 kG/GeV
Septum Thickness		8.00 mm
Deflection Angle		62.00 mrad

Figure 12j. Injection line elements.

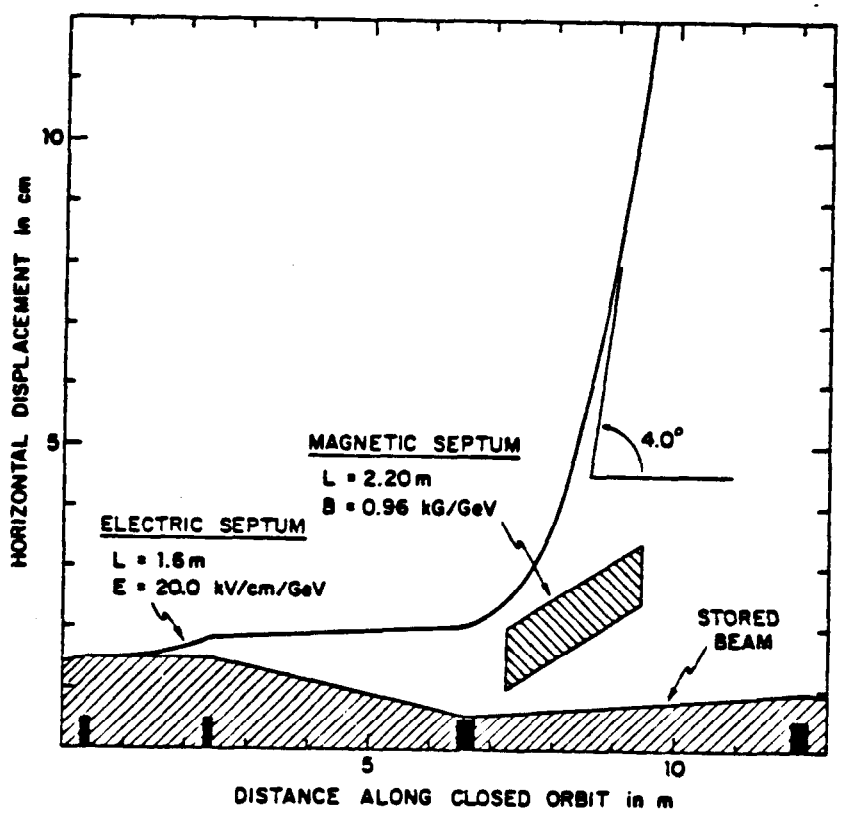

Figure 12k. Beam extraction from pulse stretcher.

Electric Septum:	
Length	1.6 m
Strength	20.0 kV/cm/GeV
Septum Thickness	50.0 μm
Deflection Angle	3.2 mrad
Magnetic Septum	
Length	2.20 m
Strength	0.96 kG/GeV
Septum Thickness	10.00 mm
Deflection Angle	63.50 mrad

Figure 12m. Extraction line elements.

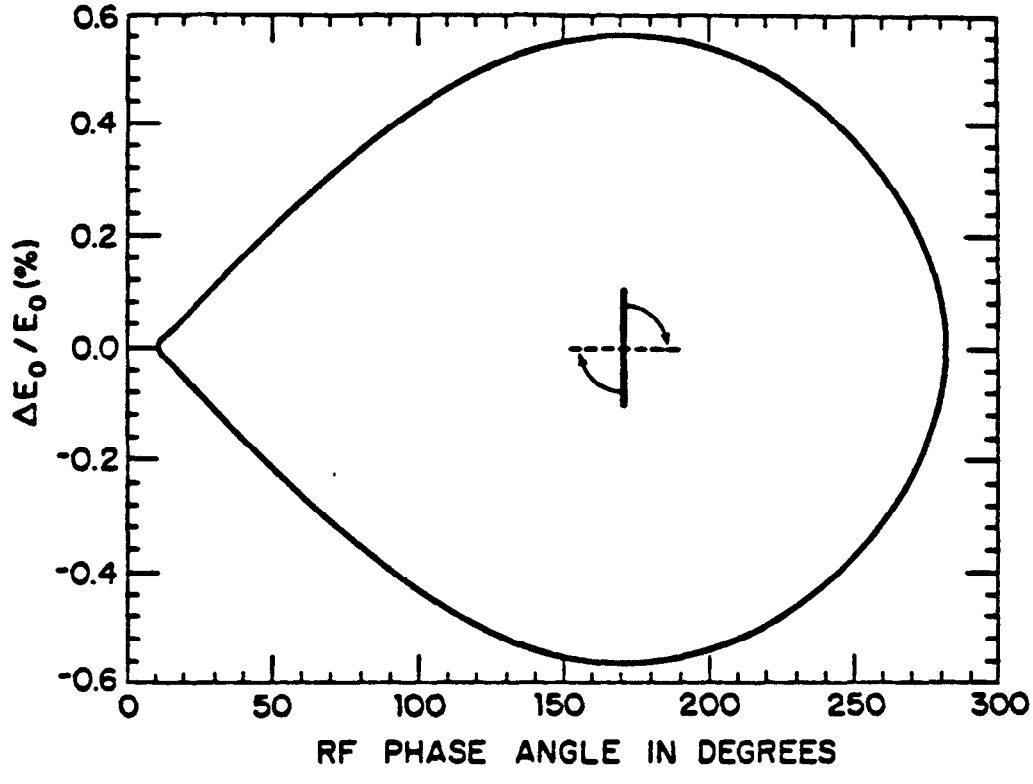

Figure 12n. Longitudinal phase space.

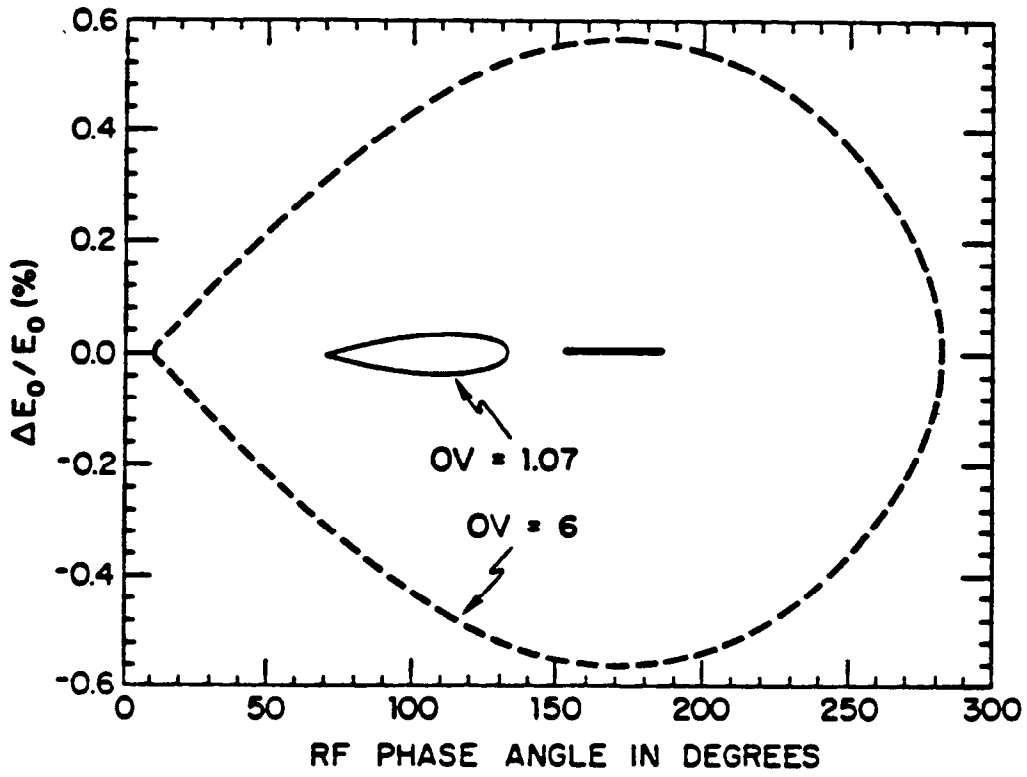

Figure 12o. RF overvoltage reduction.

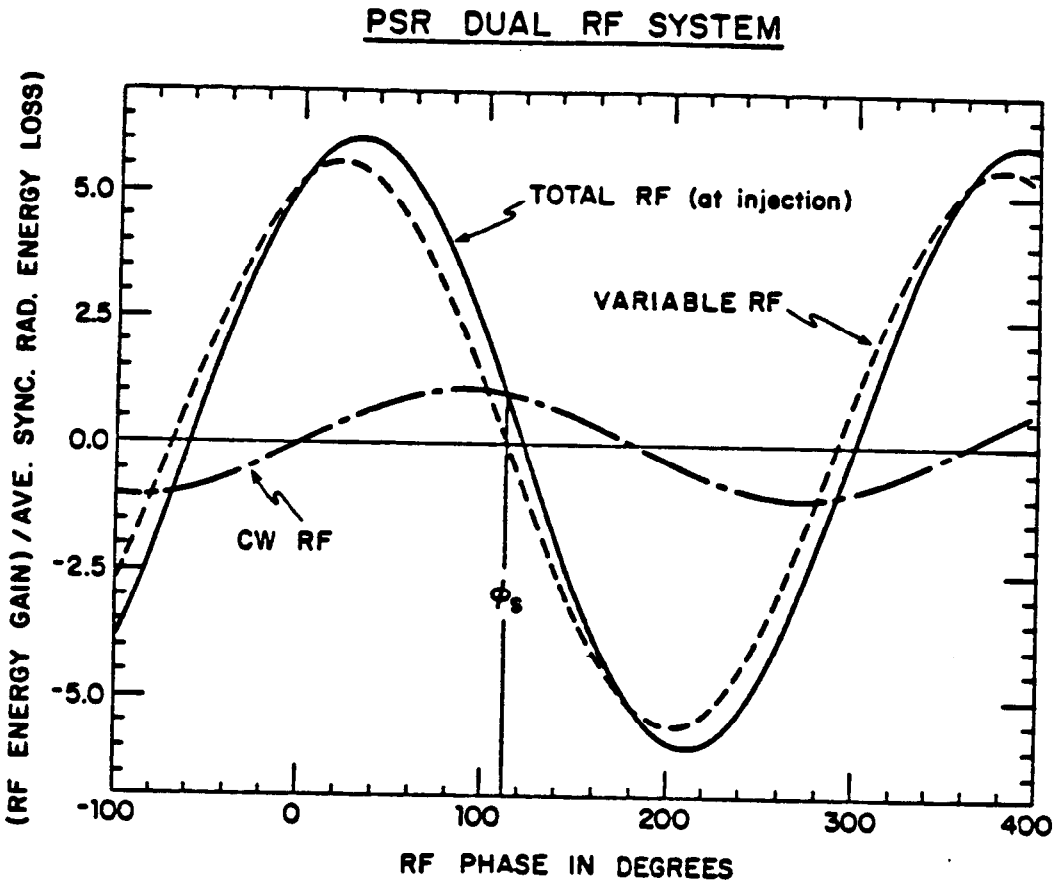

Figure 12p. Stretcher dual RF system.

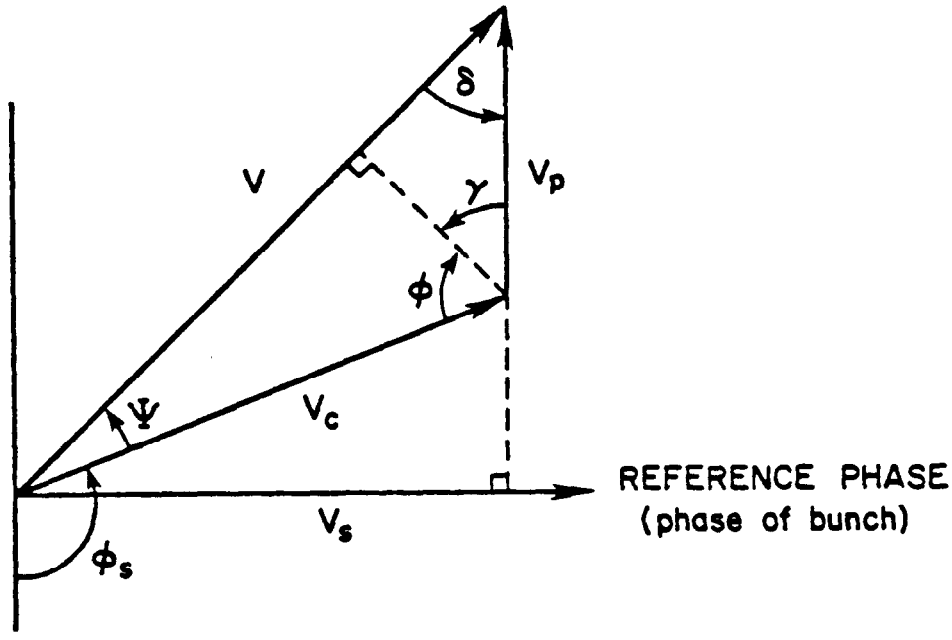

Figure 12q. Stretcher RF phase.

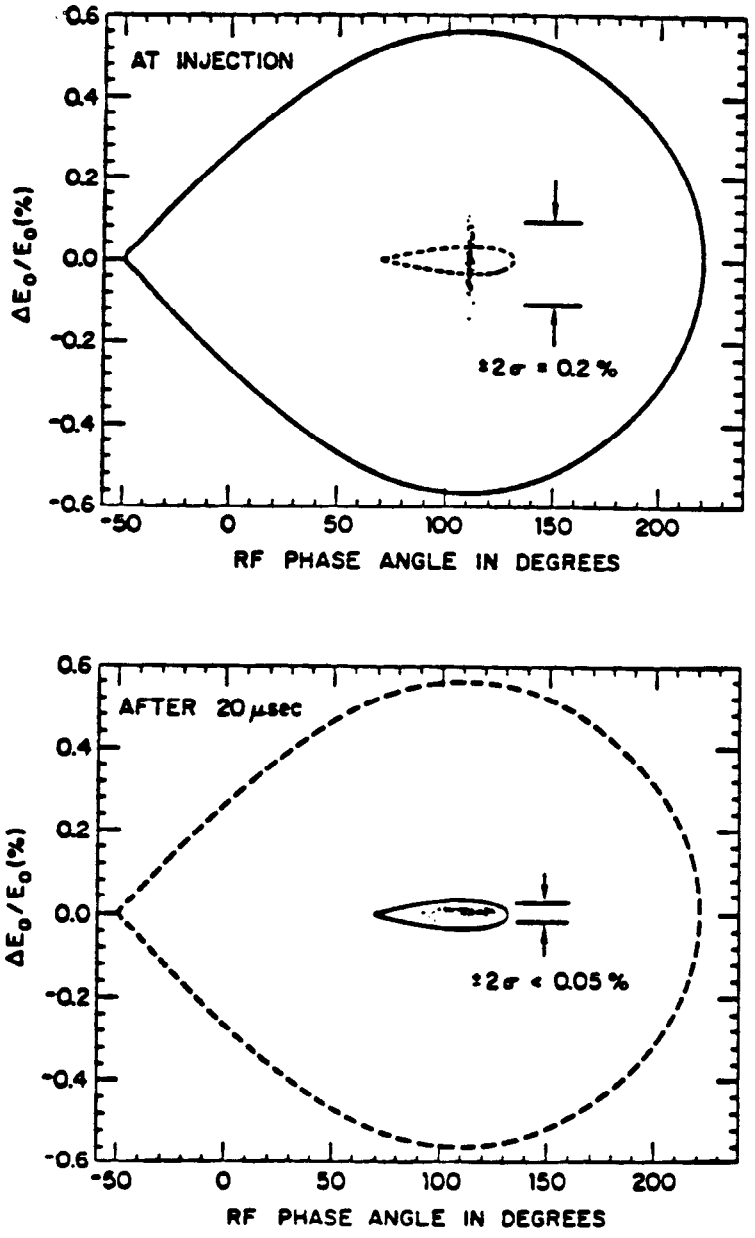

Figure 12r. Stretcher PSR energy compression at 4 GeV.

Dipoles	
Effective length	3.835 m
Width	22.0 cm
Gap	3.8 cm
Bend Angle	8.182 deg
Magnetic Radius	26.855 m
Magnetic Induction (4 GeV)	0.50 T
Number	32
Quadrupoles	
Effective length	30.0 cm
Bore	8.0 cm
Maximum Strength (4 GeV)	0.26 m^{-1}
Maximum Pole Tip Induction (4 GeV)	0.60 T
Number	30
Sextupoles	
Effective length	20.0 cm
Bore	8.0 cm
Maximum Strength (4 GeV)	0.72 m^{-2}
Maximum Pole Tip Induction	1.0 T
Number	16

Figure 12s. Basic regular bend region magnets.

Dipoles	
Effective length	3.835 m
Width	22.0 cm
Gap	3.8 cm
Bend Angle	8.182 deg
Magnetic Radius	26.855 m
Magnetic Induction (4 GeV)	0.50 T
Number	12
Quadrupoles	
Effective length	30.0 cm
Bore	8.0 cm
Maximum Strength (4 GeV)	0.26 m^{-1}
Maximum Pole Tip Induction (4 GeV)	0.60 T
Number	20

Figure 12t. Basic dispersion matching region magnets.

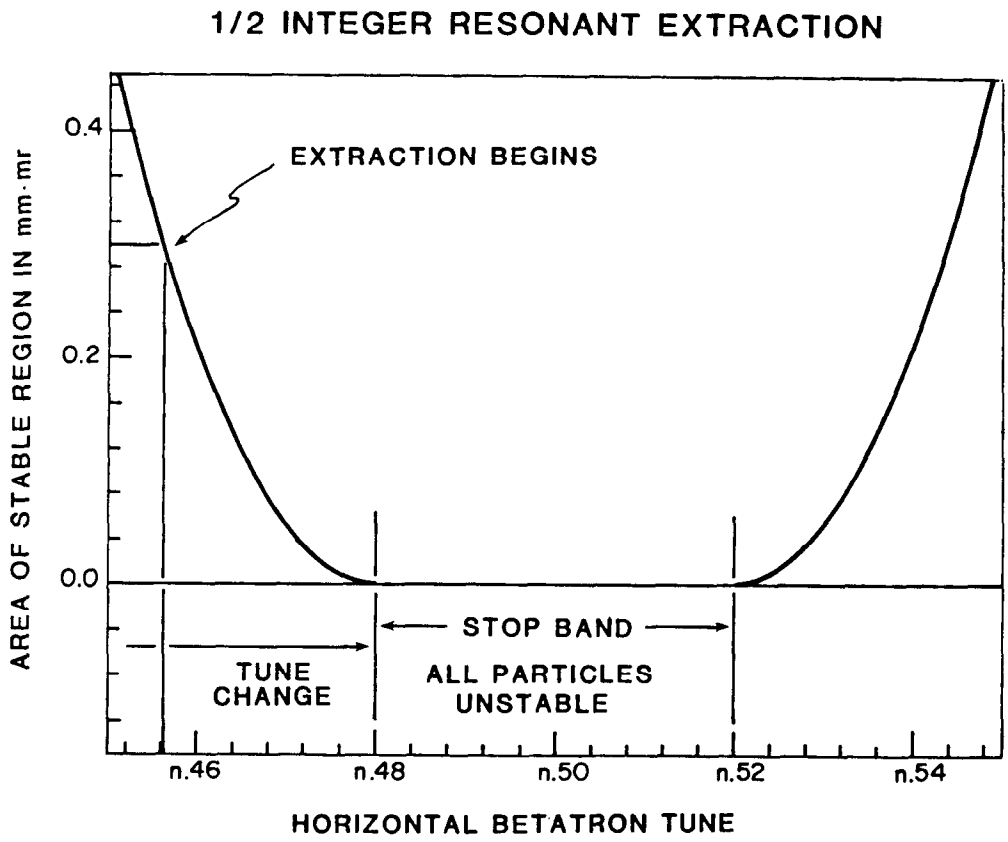
1/2 INTEGER RESONANT EXTRACTION
AREA OF STABLE REGION IN mm·mr
0.4
0.2
0.0
EXTRACTION BEGINS
STOP BAND
TUNE CHANGE
ALL PARTICLES UNSTABLE
n.46
n.48
n.50
n.52
n.54
HORIZONTAL BETATRON TUNE

Figure 12u.

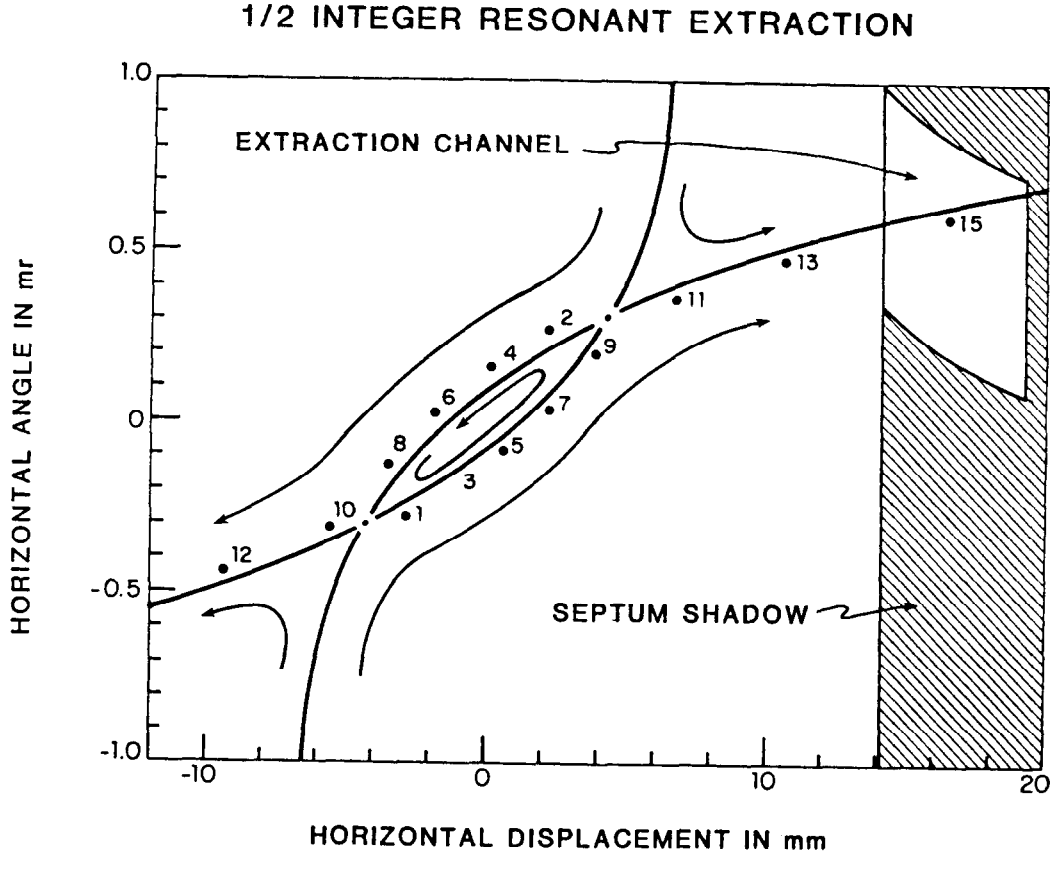
1/2 INTEGER RESONANT EXTRACTION
EXTRACTION CHANNEL
SEPTUM SHADOW
HORIZONTAL ANGLE IN mr
HORIZONTAL DISPLACEMENT IN mm
1.0
0.5
0
-0.5
-1.0
-10
0
10
20
1
2
3
4
5
6
7
8
9
10
11
12
13
15

Figure 12v.

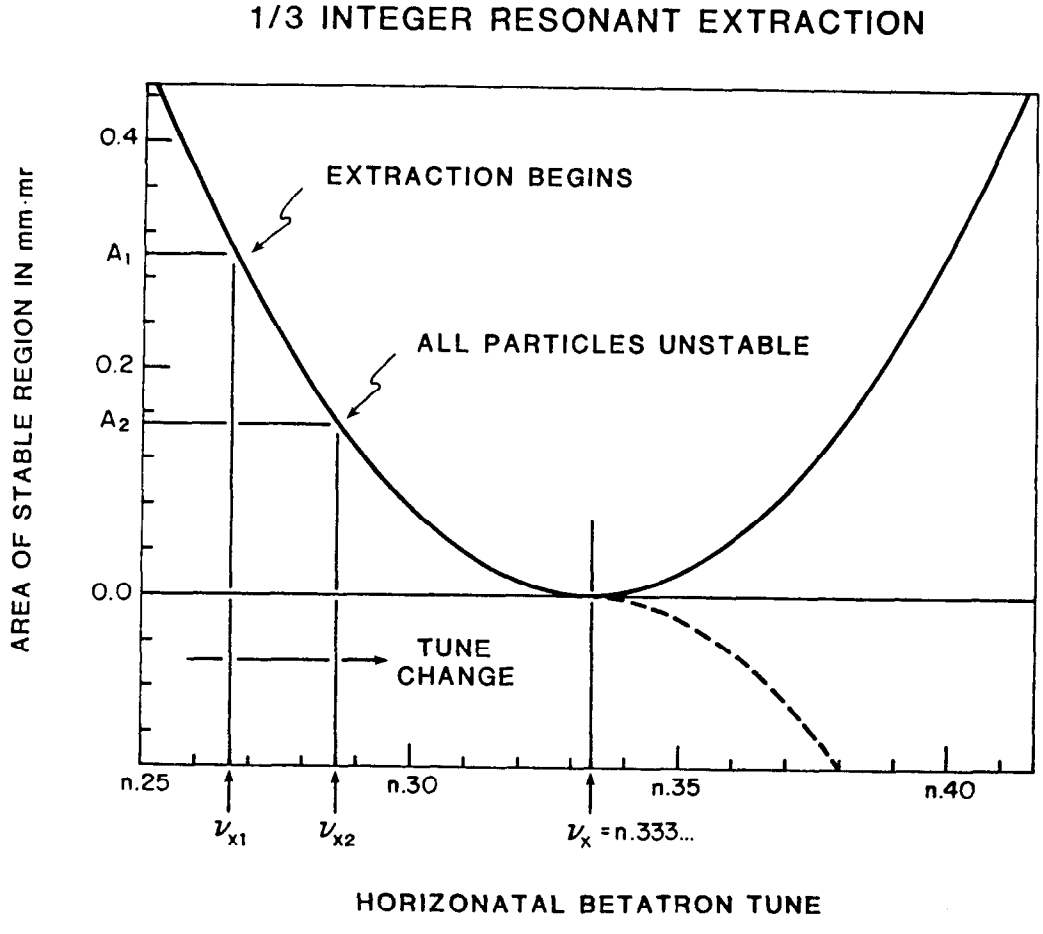
1/3 INTEGER RESONANT EXTRACTION
AREA OF STABLE REGION IN mm·mr
0.4
A1
0.2
A2
0.0
EXTRACTION BEGINS
ALL PARTICLES UNSTABLE
TUNE
CHANGE
n.25
n.30
n.35
n.40
νx1
νx2
νx = n.333...
HORIZONATAL BETATRON TUNE

Figure 12w.

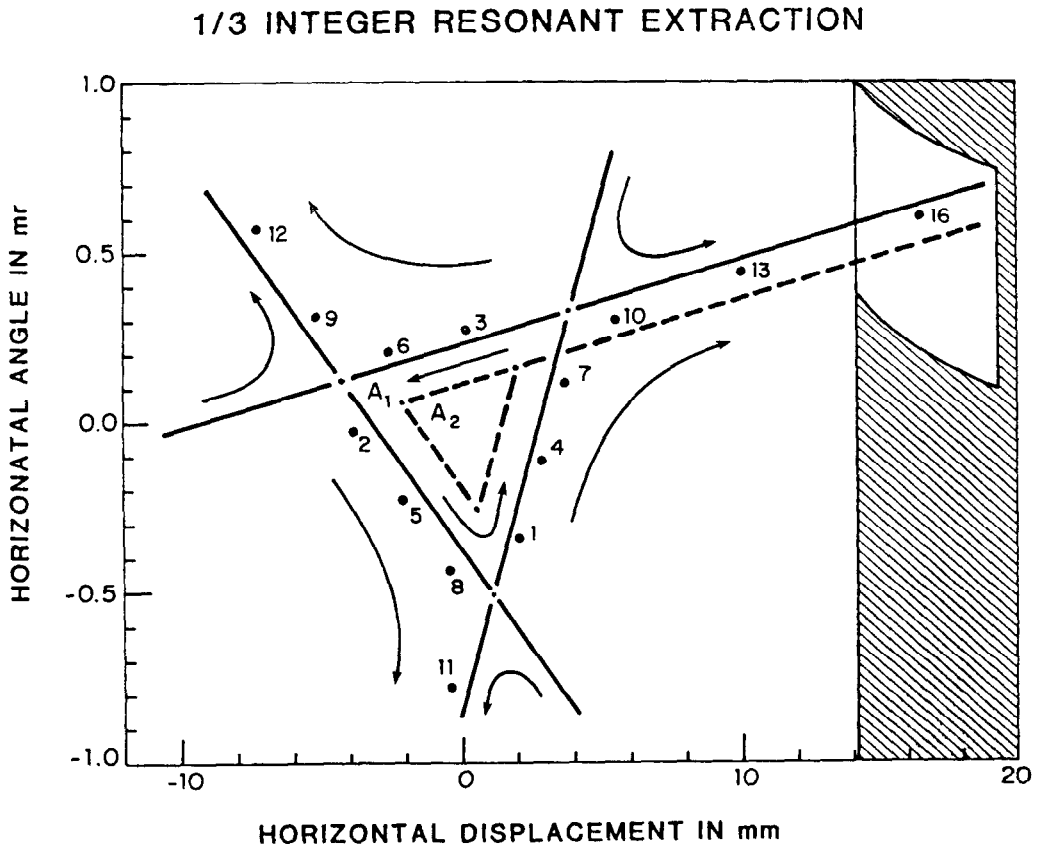
1/3 INTEGER RESONANT EXTRACTION
HORIZONATAL ANGLE IN mr
1.0
0.5
0.0
-0.5
-1.0
-10
0
10
20
HORIZONTAL DISPLACEMENT IN mm
12
9
6
3
10
16
13
7
A1
A2
2
4
5
1
8
11

Figure 12x.